6-2021

Identification and Localization of NF-κB During the Embryonic Development of the Schistosome-transmitting Snail Biomphalaria glabrata

Amanda Karin Marsh

Identification and Localization of NF-κB During the Embryonic Development of the Schistosome-transmitting Snail *Biomphalaria glabrata*

This Thesis is Presented in Candidacy for Honors at Graduation in Independent Study at Lawrence University, Appleton, Wisconsin

Amanda K. Marsh

Lawrence University ‘21

May 2021

Advisor: Judith Humphries, PhD

I hereby reaffirm the Lawrence University honor code.

Table of Contents

Abstract **3**

Introduction **4**

Background **7**

NF-κB: Overview 7

NF-κB functionality beyond immunity 11

NF-κB and B. *glabrata* studies 13

B. glabrata embryonic development 15

Investigative Approach **19**

Methods **22**

Collection and isolation of *B. glabrata* embryos 22

Immunofluorescence 23

Western Blotting 25

Results **27**

Immunofluorescence 27

p105/50 and rhodopsin immunofluorescence 27

p105/50 and phalloidin localization 36

Western Blotting 38

Discussion **40**

Conclusions and Future Studies **48**

Acknowledgements **50**

References **52**

Appendices **60**

Abstract:

The freshwater snail *Biomphalaria glabrata* is best known as the intermediate host to *Schistosoma mansoni,* a parasitic worm that causes the neglected tropical disease schistosomiasis. Because of its role as a host to a parasite, the snail can be used as a model organism to study conserved, immune-related pathways and proteins that may be involved in defense of parasite infection. One complex of proteins under investigation is nuclear factor kappa-light-chain-enhancer (NF-κB), an evolutionarily conserved family of transcription factors that are primarily known for their function in vertebrate immunity and, more recently, processes related to the nervous system. While NF-κB has been identified in adult *B. glabrata,* there are no studies examining NF-κB localization during the snail's embryonic development. In invertebrates, several studies suggest that NF-κB is a key component in developmental processes, making it plausible that *B. glabrata* utilizes the transcription factor early in its lifespan. The combination of NF-κB characterization in adult *B. glabrata* and evidence of this transcription factor's involvement in the developmental phases of several species of invertebrates led me to hypothesize that NF-κB is present and playing an active role during the embryonic stages of *B. glabrata*. In confirmation of this hypothesis, this study presents novel evidence of NF-κB localization during *B. glabrata* embryonic development using immunofluorescence and western blotting.

Introduction:

The freshwater snail *Biomphalaria glabrata* is a hermaphroditic organism native to neotropical areas in Central and South America (DeJong *et al*., 2001). Belonging to the phylum Mollusca and class Gastropoda (ITIS standard Report Page: *Biomphalaria glabrata*), *B. glabrata* is an invertebrate typically studied because it is an intermediate host-an organism where an immature form of a parasite develops- for *Schistosoma mansoni*. *S. mansoni* is a parasitic worm that causes the neglected tropical disease schistosomiasis, which affects over 230 million people globally and is the second leading cause of death by parasite, behind only malaria. Schistosomiasis is characterized by the accumulation of adult *S. mansoni* within the bloodstream. These schistosomes deposit hundreds of eggs in areas such as the liver and digestive tract. These eggs cause a granulomatous immune response by the host and the subsequent onset of the disease. A portion of the eggs are then eliminated from the body to continue the parasite's life cycle. Should defecation occur in a suitable freshwater area, the eggs will hatch to release miracidia, a larval stage suitable for infecting an intermediate snail host such as *B. glabrata*. The parasite uses the snail host to continue its maturation process until it is released into the aquatic environment in cercarial form, a free-swimming larval stage of the parasite that can travel from the intermediate host to the definitive host. Human contact with freshwater allows for cercariae to penetrate the human skin and proceed to infect the body (Fig. 1). The effects of schistosomiasis are severe, with infected individuals subjected to symptoms ranging from abdominal pain to liver enlargement (Chitsulo *et al*., 2004, Colley *et al.*, 2014).

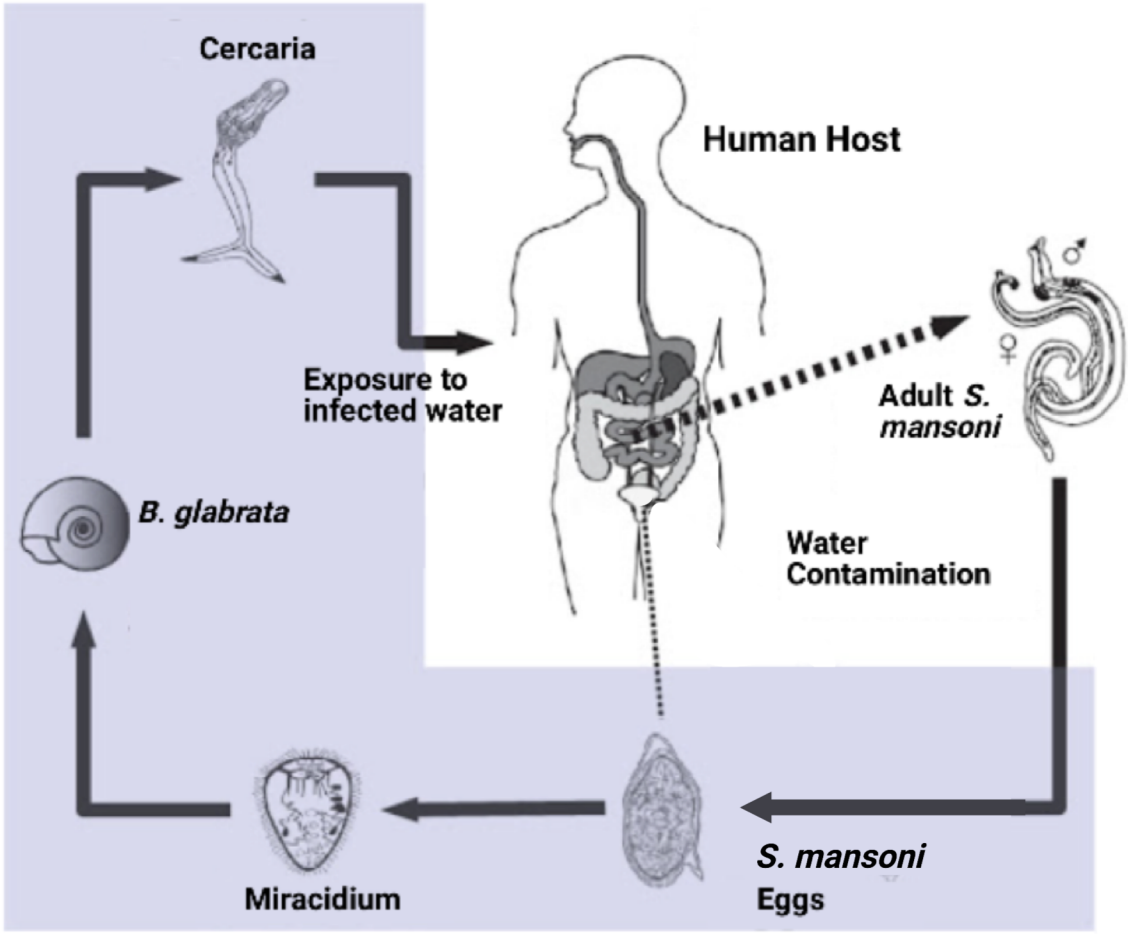

Figure 1: ***Schistosomiasis transmission cycle.*** In the human host, adult *S. mansoni* produce eggs that are defecated into a freshwater source. Following water contamination, the eggs develop into the larval stage as miracidia and are able to infect *B. glabrata.* The miracidia mature into cercarial form and emerge from the snail into the water, allowing for the parasite to infect the human host once exposed. Adapted from Mari *et al*. (2017).

Currently, there is no available vaccine to treat schistosomiasis. Instead, an orally administered drug called praziquantel has become the most widely distributed treatment, with its use dramatically increasing since its development in the 1970s due to its efficacy (Doenhoff and Pica-Mattoccia, 2006). Even so, the lack of a vaccine has proven to be a substantial roadblock in moving the number of schistosomiasis cases each year toward a negative trajectory. Without halting the transmission of *S. mansoni* in vulnerable populations, or those that use *S. mansoni*-

contaminated freshwater for daily activities, many individuals are susceptible to reinfection. Because *B. glabrata* is a host for *S. mansoni,* the snail has become a model organism for studying evolutionarily conserved pathways and mechanisms related to immunity that may be involved in defense of parasite infection.

The recent publication of the snail's genome has supplemented and enhanced studies on *B. glabrata,* providing insight into its immunological pathways (Adema *et al*., 2017). Within the past two decades, extensive studies have identified various components of the *B. glabrata* immune system, including the characterization of fibrinogen-like proteins, Toll-like receptors (TLRs), peptidoglycan recognition proteins, and recently a β pore-forming toxin (Adema *et al.*, 1997, Galinier *et al*., 2013, Adema, 2015, Pila *et al*., 2016, Adema *et al.*, 2017, Humphries and Deneckere, 2018). One of the most significant findings in identifying *B. glabrata* immune factors emerged in 2011, when Zhang and Coultas identified in adult *B. glabrata* two homologues of the nuclear factor kappa-light-chain-enhancer (NF-κB) family of transcription factors known to be involved in the regulation of vertebrate immune response. This spurred further investigations on NF-κB and its functionality in adult *B. glabrata;* however, there is still much to be learned about the role this transcription factor plays throughout this snail's life, especially during its early development.

The following study will begin with an analysis of the current knowledge of NF-κB and related proteins in *B. glabrata* as well as the role of NF-κB in invertebrate development. Knowing that there is NF-κB localization in adult *B. glabrata,* and that other invertebrates have expressed NF-κB during embryogenesis, led us to hypothesize that the transcription factor plays a role in *B.*

glabrata development. Examining when and where NF-κB emerges during the early stages of the snail's lifecycle will provide key insight into the unknown function of this protein in *B. glabrata* and thereby guide future studies on NF-κB in this species.

Background:

NF-κB: Overview

NF-κB proteins are a conserved family of transcription factors that are best known for playing a critical role in innate and adaptive immune responses in vertebrates (Li and Verma, 2002, Hayden *et al*., 2006). Transcription factors bind directly to DNA or RNA, allowing them to regulate transcription of certain genes depending on the nature of the sequence to which they attach. As a whole, NF-κB regulates over 400 genes in humans, many of which are involved in immunity. Common functions of NF-κB include regulating apoptosis, enhancing immune cell growth and proliferation, and inducing inflammation (Moynagh, 2005, Lawrence, 2009, Serasanambati and Chilakapati, 2016), all of which are essential processes in regulating immune responses and maintaining cell integrity. Recent studies also have highlighted the importance of NF-κB localization in terms of the emergence of, and response to, diseases. While NF-κB is clearly important in immunological defense, it is essential that it is functioning properly as it can be detrimental when defective. This is mainly due to the fact that many illnesses emerge from irregularities in inflammatory response and cellular proliferation, including certain types of cancers, arthritis, and muscular dystrophy (Serasanambati and Chilakapati, 2016).

The human NF-κB complex contains a total of five subunits that are encoded by distinct genes and processed. The subunits of this complex include p50, p52, RelA/p65, c-Rel, and RelB. Note that the p50, p52, and p65 proteins are named after their size in kilodaltons (kD). p50, for example, is 50 kD, p65 is 65 kD, etc. (Huxford and Ghosh, 2009). While each of these proteins may vary in function, all share a conserved 300-amino acid N-terminus called the rel homology domain (RHD) that is responsible for DNA binding at target sequences and homo/heterodimer formation to facilitate gene regulation (Rushlow and Warrior 1992, Xiao and Gosh, 2005, Hayden *et al*., 2006). p50, p52, RelA/p65, c-Rel, and RelB can be sorted into two classes: NF-κB class I (NF-κBI) and NF-κB class II (NF-κBII). NF-κBI comprises p52, p50 and their precursors p100 and p105, respectively. p100 and p105 contain a series of C-terminal ankyrin repeats, which are degraded to create p52 and p50 (Hatada *et al*., 1992). The mechanisms behind p50 production are relatively well characterized, with a glycine-rich segment and downstream ubiquitination being known to contribute to p105 processing (Cohen *et al*., 2001, Moorthy *et al.*, 2006). On the other hand, NF-κBII is made up of the rel family (RelA/p65, RelB, and c-Rel) (Baeurle and Baltimore, 1989, Gilmore, 2006). The rel family is distinguished by each member containing a transcription activation domain (TAD), whereas NF-κBI proteins lack this motif (Fig. 2). TAD is essential for targeting of gene expression and recruiting proteins that can enhance transcription rates, making NF-κBII particularly important in activating NF-κBI proteins.

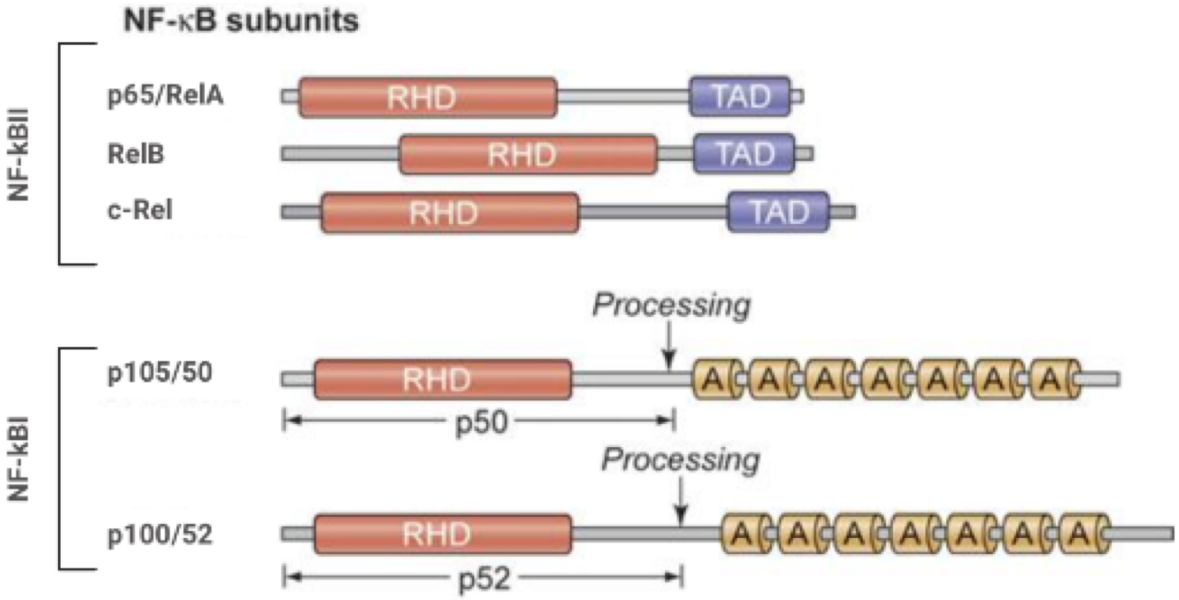

Figure 2: ***The human NF-κB subunits.*** RHD=rel homology domain, A=ankyrin repeat, TAD= transcription activation domain. Edited in BioRender. Adapted from Jost, P. J. and Ruland J. (2007).

Typically, NF-κB proteins remain inactive in the cytoplasm due to being bound by a collection of inhibitor proteins called IκBs (Kawai and Akira, 2007). One way NF-κB activation is achieved is through TLRs, a family of pattern recognition receptors that can not only identify pathogens, but also distinguish and categorize them based on moieties on the pathogen surface (Zhang and Ghosh, 2001). In this study, the pathway that NF-κB follows upon activation by TLRs will be referred to as the TLR-NF-κB pathway.

Functionally, the TLR-NF-κB pathway in vertebrates is responsible for the transcription of genes involved in inflammatory response through direct and indirect means. The pathway induces the transcription of pro-inflammatory mediators, such as cytokines, that may subsequently cause

inflammation themselves or trigger inflammatory T-cell differentiation (Hayden *et al*., 2011, Liu *et al*., 2017).

Both p50 and p65 are critical subunits in the TLR-NF-κB signaling pathway. It is important to note that alone p50 is unable to reach an activated state as it lacks the C-terminal TAD. However, other subunits, such as p65, do have this specialized domain (Fig. 2). Therefore, p50 must function as a heterodimer with p65 to create an activated complex. Together, the pair form the most commonly activated NF-κB dimer upon TLR signal induction. Activation of the p50-p65 heterodimer by TLR stimulation is accomplished by the initial phosphorylation of IκBs by the IKK kinase complex, which is made up of IKKα, IKKβ, and a NF-κB essential modifier (NEMO). IκB phosphorylation is followed by ubiquitination, or the attachment of a ubiquitin molecule to a protein that signals for the enzymatic degradation of the particular substance to which it is bound. Thus, following ubiquitination, IκB degrades and detaches from the p50-p65 heterodimer, allowing the complex to migrate to the nucleus to bind at specific DNA sequences, called κB domains, and regulate transcription (Fig. 3; Hayden *et al*., 2006, Kawai and Akira, 2007).

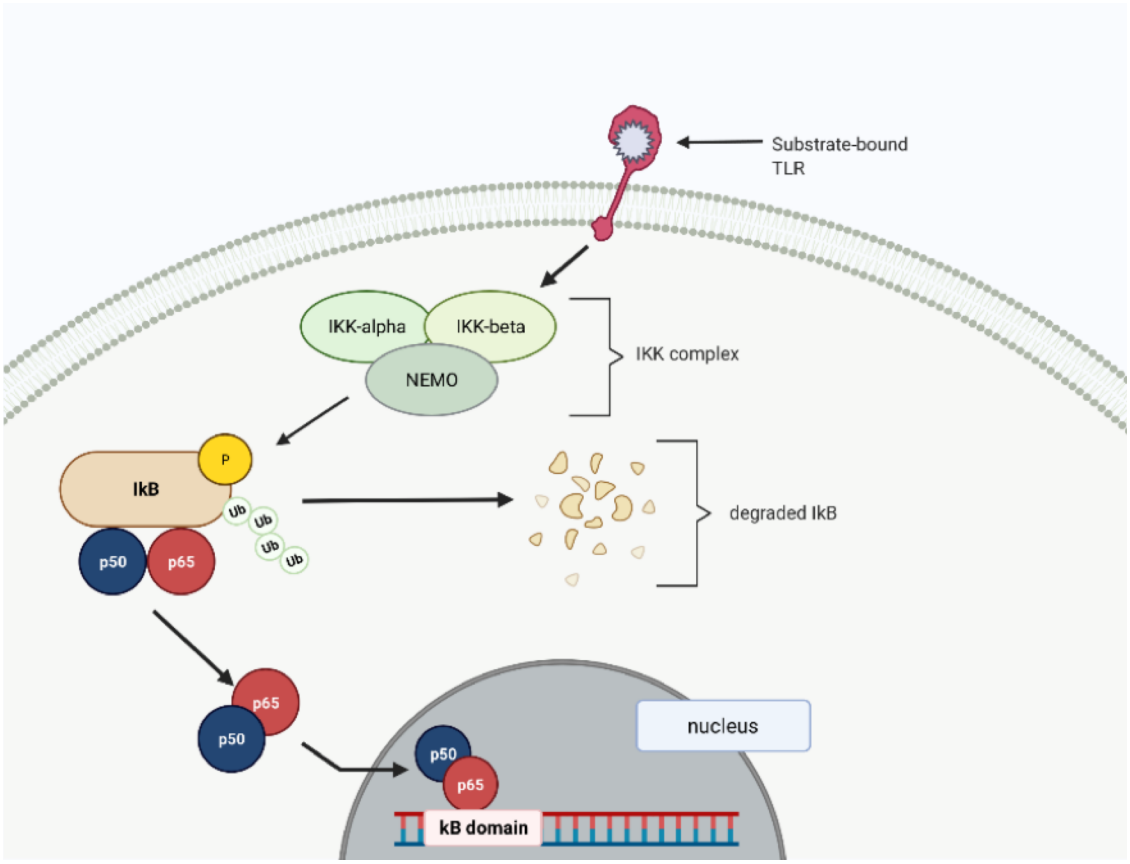

Figure 3: ***The TLR-NF-κB pathway.*** TLR binding to a pathogen substrate induces the IKK complex to phosphorylate (P) IκB, an inhibitor bound to the p50-p65 heterodimer. Ubiquitination (Ub) and subsequent degradation of IκB allows p50-p65 to migrate to the nucleus and regulate transcription by binding to a κB domain. Created through BioRender. Adapted from Abcam "Overview of the NF-κB pathway."

NF-κB functionality beyond immunity

While NF-κB is best known to regulate immune responses across a multitude of species (Hayden *et al*., 2006), studies have found that its functions may not be limited to the immune system. In addition to regulating immune responses, the TLR-NF-κB pathway has been shown to play a role in development. As of yet, there is no published research on the TLR-NF-κB pathway during molluscan development; however, several studies have emerged examining TLR and NF-κB activity during invertebrate maturation. In fact, the Toll gene, a *Drosophila* TLR homologue,

was first investigated for its role in the early stages of *Drosophila* development. It was not until later that it was also found to be involved in immunity. *Drosophila* studies also have indicated that a NF-κB homologue, Dorsal, plays a role in the development of the dorsal-ventral pattern of embryonic flies (Hong *et al*., 2008, Gerondakis and Siebenlist, 2010, Anthoney *et al*., 2018). Evidence of the TLR-NF-κB pathway functioning in development extends to other invertebrates as well, with the identification of a singular TLR in *Nematostella vectensis* (Nv-TLR) being found to colocalize with NF-κB in young embryos, confirming that TLRs and NF-κB function in similar areas. Nv-TLR was also the activator of *N. vectensis* NF-κB in human cells (Brennan *et al*., 2017), suggesting the pathway is conserved across species.

In addition to the role of NF-κB in development and immunity, over the past 25 years there has been significant evidence suggesting that NF-κB serves a wide variety of functions in the vertebrate nervous system. Notably, NF-κB has been found to be involved in neural stem cell proliferation, brain inflammation, neuronal upkeep, and synaptic functions (Kaltschmidt and Kaltschmidt, 2009). Specifically, members of the TLR-NF-κB pathway have been identified in both developing and adult mice nervous systems. In adults, p50 localized in retinal synaptic areas and p65 was found in several areas of the brain (Kaltschmidt *et al*., 1993, Meberg *et al*., 1996, Meffert *et al*., 2004, Kaltschmidt and Kaltschmidt, 2009, Fan and Cooper, 2009). Similarly, NF-κB was shown to be present in the midbrain of the developing central nervous system (CNS) in embryonic mice (Dickson *et al*., 2004), suggesting that NF-κB functioning as an immune and neurological regulator may begin in early organismal development.

NF-κB and B. glabrata *studies*

Research in infectious diseases has explored NF-κB regulation in pathogen-host relationships, including hosts infected with *S. mansoni.* Specifically, once in the human body, excretory products of *S. mansoni* have been found to inhibit NF-κB proteins from binding to certain κB domains that regulate inflammatory responses, resulting in the termination of immune cell recruitment and weakened host defense to pathogens (Trottein *et al*., 1999, Tato and Hunter, 2002). Further, a 2015 study on *S. mansoni*-infected mice found that NF-κB and TLR levels were significantly elevated during the host's immune response to the parasite. As a result, NF-κB is being examined as a therapeutic target for future anti-schistosomiasis drug development (Ashour *et al*., 2015). However, there is still much to be learned about NF-κB in *B. glabrata* as a whole before determining its role in parasite defense.

Given the critical role of *B. glabrata* as an intermediate host in the *S. mansoni* lifecycle and the importance of NF-κB in parasite-host interactions, it is of great interest to fully examine the possible functions and localization of the TLR-NF-κB pathway in *B. glabrata.* While portions of the TLR-NF-κB pathway have been characterized in mollusks (Montagnani *et al*., 2004, Goodson *et al*., 2005, De Zoysa *et al*., 2010), Zhang and Coultas (2011) were the first to identify and characterize NF-κBI and II in adult *B. glabrata* specifically. This ultimately ignited further investigation of NF-κB in the snail. Most importantly, however, their identification of NF-κBI and II pointed to the likelihood of the entire TLR-NF-κB pathway being in *B. glabrata.* Thus, in subsequent years following the publication of Zhang and Coultas' study, several putative portions of the TLR-NF-κB pathway were discovered in adult *B. glabrata* including TLRs and

κB domains (Humphries and Harter, 2015, Adema *et al*., 2017, Humphries and Deneckere, 2018).

From recent studies on NF-κB in adult *B. glabrata,* it can be hypothesized that NF-κB does in fact serve some kind of function in the immune and nervous systems in the snail as it does in vertebrates. Research conducted by Humphries and Harter (2015) identified several κB domains in *B. glabrata* to which the RHD of the *B. glabrata* p65 homologue bound to. Uniquely, these particular κB domains were found just upstream of the p38 mitogen–activated protein kinase (MAPK) and IκB. p38 MAPK is one of several subgroups in a family of kinases that are involved in signal transduction regulation, inflammation, and NF-κB processing (Zarubin and Han, 2005). It has been determined that p38 MAPK regulates acetylation of p65, or the addition of an acetyl group to a protein to facilitate its activity (Saha *et al*., 2007). NF-κB binding to domains upstream of these immune-related genes ultimately suggests that the transcription factor likely serves a related function in immunity in *B. glabrata*. Because the function of NF-κB in vertebrates is well characterized as having a regulatory effect on immunity, it is important to note that the *B. glabrata* RHD of p65 was able to bind to vertebrate κB domains as well. This suggests that the process of p65, and possibly other NF-κB proteins, binding with κB domains is conserved across species (Humphries and Harter, 2015). Later research in the Humphries Lab further supported this initial finding, with identification of several additional κB domains upstream of several members of the TLR-NF-κB pathway, suggesting that NF-κB may be regulating a portion of that pathway (Humphries and Deneckere, 2018). While there have not been any investigations of NF-κB functionality in the *B. glabrata* CNS, preliminary immunochemical studies of p50 showed immunoreactivity in the adult *B. glabrata* brain (Judith

Humphries, PhD, personal communication), suggesting that p50 may be active in the snail's CNS as it is in other species.

As studies on the TLR-NF-κB pathway in *B. glabrata* continue to accumulate and suggest that it may serve immunological and neurological functions in the snail, it is important to note that this research has only been conducted in adult *B. glabrata*, leaving NF-κB localization during embryogenesis unstudied. Thus, there is a gap in our understanding of whether NF-κB functions in *B. glabrata* embryos, and if so, how.

B. glabrata *embryonic development:*

There are few published studies documenting the stages of *B. glabrata* embryogenesis. To date, the most thorough analysis of the snail's development comes from the research of Camey and Verdonk (1970). However, certain details of *B. glabrata* growth, particularly later embryonic stages, were absent from this study and must instead be characterized by conserved patterns of embryogenesis in related gastropods that have been more extensively studied, such as *Lymnaea stagnalis*. Like *B. glabrata, L. stagnalis* is an intermediate host for parasites and can be used as a model organism to fill gaps of knowledge in *B. glabrata* embryogenesis (Kuroda and Abe, 2020). For the purposes of this study, however, all analysis of snail embryogenesis will be specific to *B. glabrata* until otherwise noted.

As in other pond snails, development of *B. glabrata* begins with the initial laying of egg masses, characterized by clusters of embryos in individual chambers (Croll, 2009). The embryos will

grow and develop for 6-7 days before undergoing metamorphosis and emerging from their chambers in young-adult form. Between the time of fertilization and leaving the egg mass, *B. glabrata* embryogenesis is characterized by five distinct developmental stages: blastula, gastrula, trochophore, veliger, and finally juvenile. To supplement and enhance the work of Camey and Verdonk (1970), Lulu Bautista-Ruiz of the Humphries lab documented and photographed these stages of embryonic development in *B. glabrata* (Fig 4).

The blastula stage is the first period of *B. glabrata* development and occurs during the initial 0-2 days following fertilization when the egg masses are laid. This stage is characterized by notable cleavage of cells, beginning with the initial splitting of the single-celled egg (Fig. 4A). After at least three series of cell division, the embryo transitions into the gastrula phase around day 2 post-fertilization. It is during this stage that the cells are seen in distinct germ layers, which are visually identified by a contrast in cell density and therefore color when observing the embryo. Further, the blastopore, or the initial embryonic opening that creates the anus or mouth in an organism, can also been seen during gastrula (Fig. 4B). During days 2-3 of development, the embryos enter the trochophore stage. There are two notable events that occur during this time of development. The first is the emergence of the visceral mass, which will later develop into the snail's organs. The second is that the embryos express movement for the first time in the form of stationary revolutions in their chambers (Fig. 4C).

Following the trochophore stage, *B. glabrata* embryos undergo the second to last stage of embryogenesis, the veliger. The veliger stage occurs over a longer period of time compared to other stages as it lasts between days 4-6 of development. This prolonged time of development

can be divided into three stages: early, middle (mid), and late veliger. During early veliger, in addition to the growth of the visceral mass, the beginnings of the shell, the radula, or feeding organ, and the headfoot region begin to form. The headfoot comprises the muscle tissue by which the snail moves, the "foot," as well as the sensory organs that make up the "head," such as the eye spots, tentacles, and the CNS. However, in early veliger, the headfoot is only just becoming visible as a uniform, translucent shape protruding from the visceral mass. There are minimal differences between early and mid-veliger, as mid-veliger mainly consists of the growth and elongation of the headfoot, shell, and visceral mass. An indicator of the transition from early to mid-veliger, however, is the initial budding of the tentacles that will later grow into long, thin structures used for environmental and spatial sensing. The final portion of the veliger stage, late-veliger, is characterized by enhanced distinctiveness between the shell and headfoot. The tentacles continue to protrude from the headfoot near the shell opening, and the eye spots, although not visible in Figure 4D, also develop at the base of the tentacles (Fig. 4D). *B. glabrata* embryogenesis concludes with the juvenile stage, occurring between 6-7 days post-fertilization. Camey and Verdonk did not characterize *B. glabrata* embryos at this stage; however, observations of the snail show similar characteristics to juvenile *L. stagnalis*. The snail grows to fill most of the chamber and darkens in color. The juvenile looks similar to a young adult with a prominently defined shell and headfoot (Fig. 4E, F) and is ready to hatch during this time period (Boyce *et al*., 1967, Camey and Verdonk, 1970, Bautista-Ruiz, 2020).

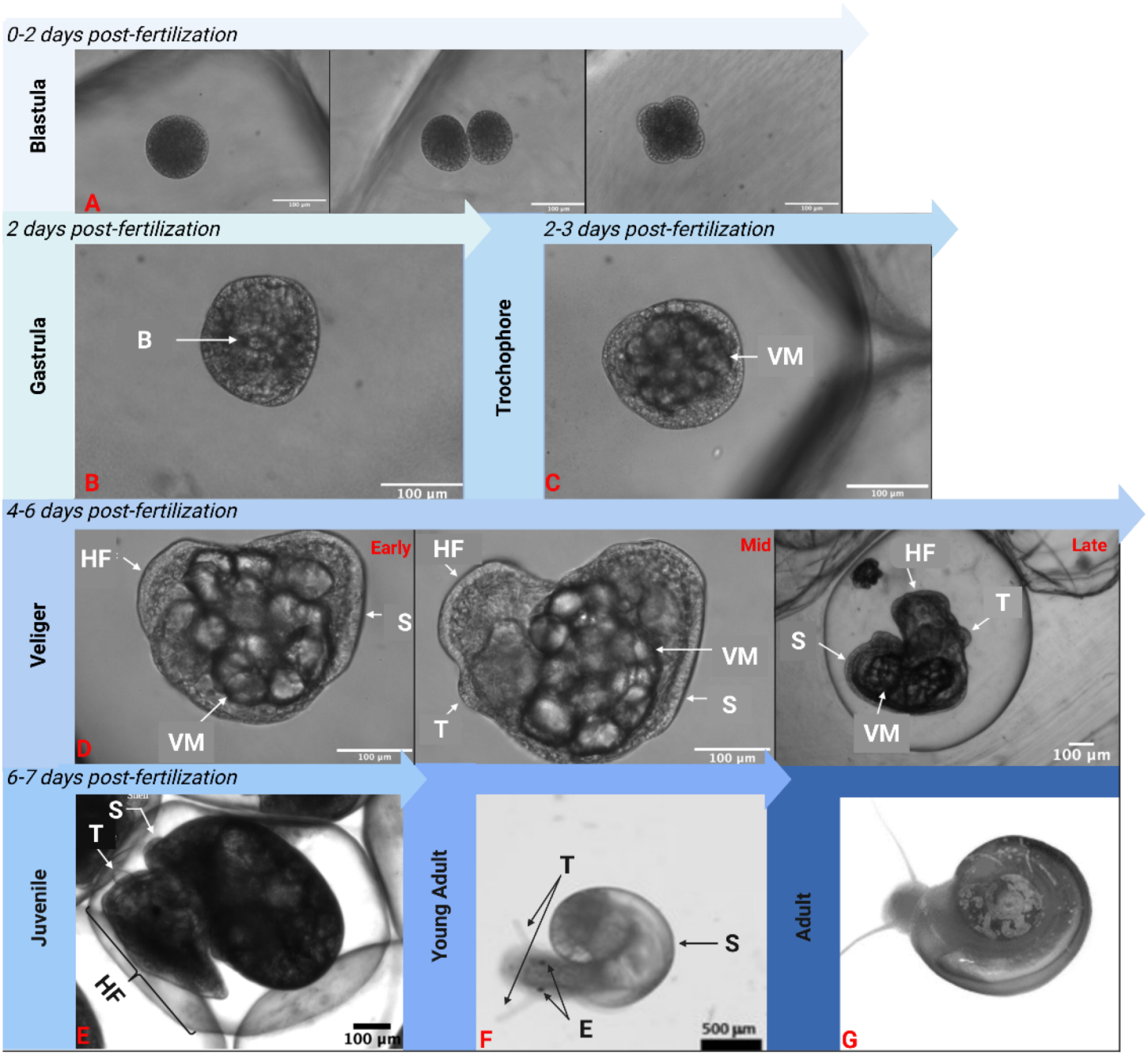

Figure 4: ***Developmental stages of*** **B. glabrata**. (A) Initial cell cleavages during the blastula stage. Note that not all series of division that may occur during this stage are documented. (B) Gastrula embryo. (C) Trochophore embryo. (D) Veliger stages: Embryos marked as "early," "mid," and "late" veliger phase. (E) Juvenile embryo immediately prior to hatching. Newly post-embryonic *B. glabrata* are noted as young-adults (F) and fully mature snails are deemed as adults (G). B=blastopore. VM=visceral mass. HF=headfoot. S=shell. T=tentacle. E=eye spots. Figures A-E adapted and complied from Bautista-Ruiz (2020). Figure F adapted from Araújo *et al.* (2020). Figure G adapted from Kenny *et al*. (2016). Completed and compiled figure constructed in BioRender.

Investigative Approach:

Studies on NF-κB in *B. glabrata* have been limited despite advances made in characterizing various components in the TLR-NF-κB pathway over the past decade (Zhang and Coultas, 2011, Humphries and Harter, 2015, Adema *et al*., 2017, Humphries and Deneckere, 2018). This is especially true in regard to investigations of NF-κB during *B. glabrata* embryonic development. In fact, there has yet to be any identification or research to emerge on whether the TLR-NF-κB pathway is active during the gastropod's early life stages. However, the combination of known NF-κB expression in adult *B. glabrata* and evidence of NF-κB in early invertebrate development catalyzed the aim of this study-to investigate possible NF-κB localization and functionality during *B. glabrata* embryogenesis for the first time and therefore increase knowledge of this transcription factor during the snail's early life.

To conduct this study, a custom antibody was created in rabbits against the N-terminus of p105/50 (Pacific Immunology, Ramona, CA), one of the characterized NF-κB proteins in *B. glabrata*. While p50 is the proteolytic product of p105 (Gilmore, 2006), both p105 and p50 contain the same N-terminal antigen (Fig. 2), making p105/50 a target for the antibody alike. Specifically, the p105/50 antigen represents the N-terminal amino acids 2-22 (SSYGSSSNDSDTLNENNLPVD-cys). While this sequence was obtained from adult *B. glabrata*, it is assumed that if present in embryos the p105/50 sequence would be the same (Kenny *et al*., 2016), suggesting that the p105/50 antibody would precisely detect p105/50 in developing *B. glabrata*. Using a lab population of *B. glabrata* embryos of the BS-90 strain

ranging from 0 days old (immediately post-fertilization) to 7 days old (immediately prior to hatching) were collected as the experimental groups. Rather than separate embryos by individual days of development, the snails were deemed to be 0-1 days, 1-2 days, 2-3 days post-fertilization, etc. as it was impossible to determine the exact time that the snails laid the egg masses. However, it is important to note that each group of embryos was in a similar stage of development regardless and categorizing them in this way effectively captures embryogenesis in its entirety. Two primary methods, immunofluorescence and western blotting, were used to investigate possible p105/50 localization and expression at each stage of development.

The approach used for immunofluorescence in this study followed a typical protocol for indirect immunofluorescence. While direct immunofluorescence entails the direct binding of a fluorophore-tagged antibody to a protein of interest (Fig. 5), in indirect immunofluorescence, embryos are first treated with a primary antibody to bind to the desired target and are later incubated with a secondary antibody containing a fluorescent tag to allow for microscopic visualization of immunoreactivity (IR; Fig. 5). The main benefit of using immunofluorescence is that the spatial location of a protein's IR can be observed, which can help identify the function of the protein, as well. In an attempt to determine if p105/50 localized in certain areas of *B. glabrata* embryos, additional reagents known to target structures such as muscle and photoreceptors were therefore utilized.

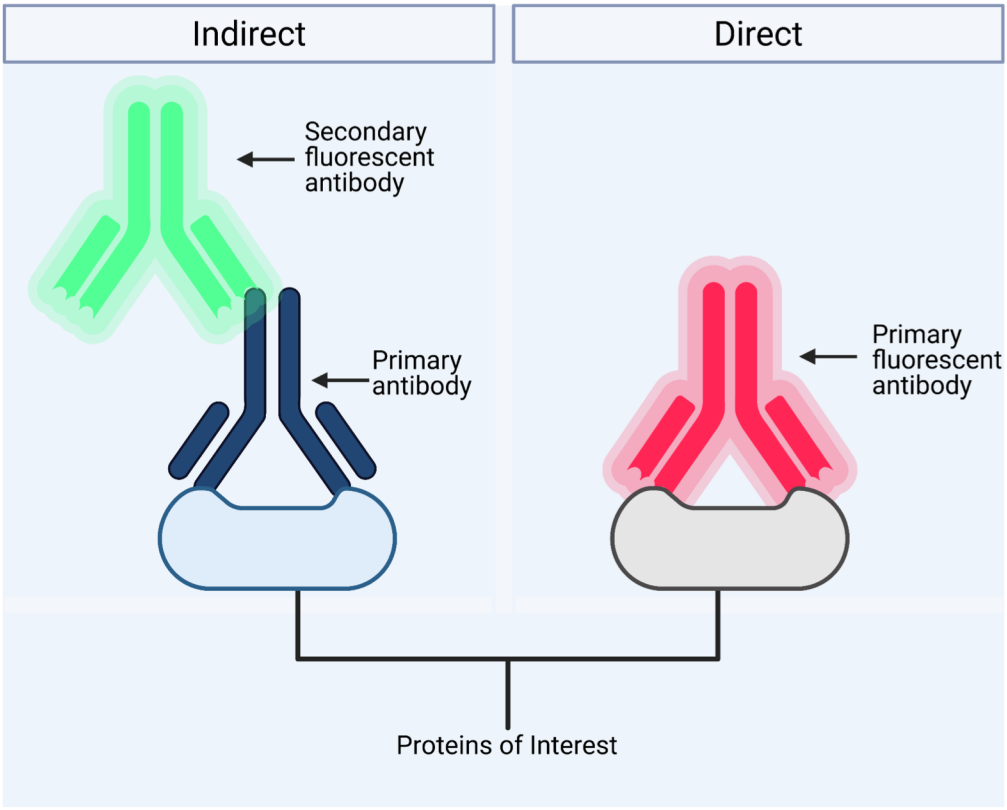

Figure 5: ***Schematic of indirect vs direct immunofluorescence.*** In indirect immunofluorescence (left), the protein of interest is initially bound to its corresponding primary antibody. A fluorescent secondary antibody is then attached to the primary antibody to allow for microscopic visualization. In direct immunofluorescence (right), a fluorescent antibody is bound directly to the protein of interest. Created in BioRender.

Further, western blotting was used to supplement any p105/50-IR seen. Importantly, western blotting can ensure that the p105/50 antibody is binding to the correct protein by showing a band at the expected weight of the cleaved p105 subunit (50kD).

This experimental study will investigate NF-κB localization and expression in early *B. glabrata* development and provide a foundation for future research that will investigate more thoroughly not just the purpose of NF-κB during the embryonic portions of the snail's life cycle, but also

how its expression and function change over time. This enhanced knowledge regarding the localization and functionality of *B. glabrata* NF-κB will support future studies investigating the possible role of NF-κB in other mollusks.

Methods

Collection and isolation of B. glabrata *embryos*

A population of BS-90 *B. glabrata* snails were kept at a temperature of 26°C on a 12-hour light/dark cycle in shallow glass dishes filled with artificial pond water (1.25mM $CaCO_3$, 3.75mM $MgCO_3$, 5.25mM NaCl, and 0.75mM KCl in aged tap water). The snails were fed romaine lettuce *ad libitum* and the tanks were cleaned once a week. To collect embryos, a small piece of polystyrene (~1x1in) was placed in the dish as a substrate for egg laying and then monitored for the presence of eggs every 12 hours. Once laid, egg masses were placed in a separate dish of artificial pond water and left to develop. At the desired stage of development, between 0-7 days post-laying, the egg masses were removed from the polystyrene using a scalpel and then placed in a petri dish containing artificial pond water. While viewing with a Nikon SMZ745 dissection microscope (Nikon Instruments Inc., Melville, NY), individual embryos were isolated from the egg masses using beading needles. Isolated embryos were then treated according to immunofluorescence or western blotting protocols

Immunofluorescence

To determine if p105/50 was present in *B. glabrata* embryos, indirect immunofluorescence was used as a primary method for visual observation of p105/50-IR. Isolated embryos to be used for indirect immunofluorescence were fixed in 4% paraformaldehyde (PFA) in phosphate buffered saline (PBS, 0.14M NaCl, 2.7mM KCl, 10mM NaH_2PO_4, 1.8mM KH_2PO_4, pH 7.4) for approximately 2 hours at 4°C. Following fixation, embryos were washed once with 4% Triton X-100 (TX) in snail PBS (sPBS; 8.41mM Na_2HPO_4, 1.65mM NaH_2PO_4, 45.34mM NaCl, pH 7.4) and then stored in sPBS at 4°C for future use.

Two primary antibodies were used for indirect immunofluorescence; one against *B. glabrata* p105/50 and another against rhodopsin. The first was a custom antibody against the N-terminus of *B. glabrata* p105/50 that was produced in rabbits (Pacific Immunology). Specifically, the antigen was amino acids 2-22 (SSYGSSSNDSDTLNENNLPVD-cys) and serum was affinity purified prior to use. The second antibody was anti-rhodopsin (Cosmo Bio Co., Carlsbad, CA), which was previously reported to successfully bind rhodopsin in another freshwater snail *L. stagnalis* (Takigami *et al*., 2014). For each antibody, working concentrations were optimized for anti-p105/50 and anti-rhodopsin reagents; however, the protocols for indirect immunofluorescence were otherwise identical.

Prior to incubation with antibodies, 5-7 day old embryos were treated with 0.5% trypsin from porcine pancreas (Sigma-Aldrich, St. Louis, MO) in sPBS for 1 minute, and were subsequently washed 4 X 15 minutes with 4% TX in sPBS (sPBS-TX). Embryos younger than 5 days, which are structurally more fragile than their older counterparts, were not treated with 0.5% trypsin.

Regardless of the stage of development, all embryos were subsequently incubated in 5% bovine serum albumin (BSA; Sigma-Aldrich) in sPBS, overnight at 4°C. 5% BSA served as the primary blocking diluent throughout the experiment unless otherwise noted and prevented nonspecific antigen binding.

Following blocking, embryos were incubated in either anti-p105/50 (Pacific Immunology; 0.5µg/mL) or anti-rhodopsin (Cosmo Bio Co.), which was diluted according to the manufacturer's recommendations (1:4000) as the concentration of the antibody was not provided. Embryos incubated with anti-p105/50 or anti-rhodopsin antibodies overnight at 4°C and were then washed 4 X 15 minutes in sPBS-TX. Following washing, embryos were incubated with a fluorophore-tagged secondary antibody, anti-rabbit Alexa 488-conjugated IgG (Cell Signaling Tech., Boston, MA; 1:2000), and protected from light overnight at 4°C. The next day, the embryos were again washed 4 X 15 minutes in sPBS-TX and mounted onto glass slides with Vectashield mounting medium (Vector Laboratories Inc., Burlingame, CA).

As a control, embryos were not treated with any primary antibody and were instead only incubated with anti-rabbit Alexa 488 with otherwise the same protocol. This control supports the specificity of any observed IR as it determines whether the secondary antibody bound only to primary antibodies (anti-p105/50 and anti-rhodopsin) or to tissue directly.

In addition to anti-p105/50 and anti-rhodopsin antibody treatments, which used indirect immunofluorescence methods, embryos were also incubated with Alexa Fluor 555-conjugated phalloidin (Cell Signaling Tech.), an actin-binding reagent. All embryos were subjected to the

same initial trypsin and blocking treatments as the embryos incubated with primary antibodies, however, as phalloidin is directly tagged to Alexa Fluor 555, a secondary reagent was not required. Therefore, embryos were incubated in Alexa Fluor 555 phalloidin in sPBS (1:20) at room temperature for 15 minutes, washed 1 X 15 mins with sPBS, and subsequently mounted onto glass slides with Vectashield mounting medium (Vector Laboratories Inc.) for viewing.

All treated embryos were viewed using a Leica DM1000 LED microscope and imaged using a Leica TCS SP5 II confocal microscope (Leica Microsystems Inc., Buffalo Grove, IL).[1]

Western Blotting

In addition, western blotting was used to determine whether p105/50 is expressed during embryonic development and to further support any p105/50-IR seen though immunofluorescence. Isolated embryos to be used for western blotting were homogenized in sPBS and centrifuged at 13,200 rounds per minute (rpm) for 2 minutes at 4°C. The supernatant was then collected and stored at -80°C for future use.

Samples of *B. glabrata* embryos between 2-7 days of development were collected and isolated as described above. In addition to embryos, two controls were utilized. The first was created using a sample of adult *B. glabrata* tissue, which is known to express p105/50 (Zhang and Coultas, 2011). The headfoot of an adult BS-90 snail was homogenized in sPBS and subsequently centrifuged at 13,200 rpm for 2 minutes at 4°C. The supernatant was then collected and stored at

[1] For details regarding the settings used for image acquisition, see Appendix I: Methods Expanded.

-80°C for future use. To confirm the specificity of the p105/50 antibody being used, an additional control group was created using a recombinant *B. glabrata* p105/50 protein.[2] To measure the levels of protein in each sample, a BCA protein assay was carried out according to the manufacturer's instructions (Pierce BCA Protein Assay Kit, Thermo Scientific, Waltham, MA).[3] A BCA protein assay assisted in assuring that the same amount of protein was loaded into each well of the gel. Thus, p105/50 expression could be monitored throughout development by examining changes in band intensity between each sample; if band intensity varied, differences in total protein concentration could be eliminated as the cause.

In preparation for SDS-PAGE, 2-7 day embryonic, adult, and purified recombinant p105/50 protein samples were thawed over ice. 10µg total protein in embryonic and adult samples and 2.5µg total protein in recombinant p105/50 protein samples were mixed with 2x Laemmli sample buffer (Bio-Rad, Hercules, CA) and boiled at 95°C for 5 minutes in an Eppendorf thermal cycler (Sigma Aldrich). Samples were subsequently cooled on ice to room temperature. SDS-PAGE was conducted by loading samples into a 10% Mini-PROTEAN TGX Precast Protein Gel (Bio-Rad) and run in 1x running buffer (25 mM Tris, 192 mM glycine, 0.1% SDS, pH 8.3) within a Mini-PROTEAN Tetra cell (Bio-Rad). Following SDS-PAGE, the protein was transferred onto a nitrocellulose blotting membrane (GE Healthcare, Marlborough, MA) in 1x transfer buffer (25 mM Tris, 129 mm glycine, 20% methanol, pH 8.3). Following, the membrane was blocked in 5% BSA in 0.1% tween-tris-buffered saline (TBS-T; 200 mM Tris, 1.5 M NaCl, pH 7.6) overnight at 4°C. The following day, the membrane was incubated with p105/50

[2] For details regarding the creation of the purified *B. glabrata* p105/50 purified protein, see Appendix I: Methods Expanded

[3] For further information regarding the methodology of the BCA protein assay, see Appendix I: Methods Expanded.

antibody in 5% BSA in 0.1% TBS-T (10μg/mL) and gently rocked for 2 hours. After primary antibody incubation, the membrane was washed with 0.1% TBS-T 2 X 15 minutes. Next, a secondary solution of anti-rabbit IgG AP-linked antibody (Cell Signaling Tech.) in 5% BSA in 0.1% tween-TBS (1:7500) was added to the membrane and was left to rock for 1 hour. Once again, the membrane was washed with 0.1% tween-TBS 2 X 15 minutes. After secondary incubation, the membrane was briefly rinsed with alkaline phosphatase buffer (AP buffer; 100mM Tris-HCl [pH 9.0], 150 mM NaCl, 1mM $MgCl_2$) before being treated with a solution of 5-bromo-4-chloro-3-indolyl-phosphate/nitro blue tetrazolium (BCIP /NBT) development substrate (Promega, Madison, WI) in AP buffer.[4] The membrane was left to develop until bands became visible near 50 kD that would correspond to p50, the cleaved form of p105.

Results

p105/50 and rhodopsin immunofluorescence B. glabrata

The aim of this study was to examine whether p105/50 is expressed during *B. glabrata* development through immunofluorescence and western blotting. Utilizing immunofluorescence, embryos were examined for p105/50-IR at 0-7 days post-laying. There was no noticeable p105/50-IR in earlier stages of embryonic development, specifically prior to 4 days post-laying (Fig. 6A-D). However, beginning at 4 days of development, p105/50-IR was observed in the

[4] For information regarding the creation of the BCIP /NBT development substrate, see Appendix I: Methods expanded.

snail's eye spot (Figs. 6E, 10A). At this stage of development, however, there was no distinguishable p105/50-IR outside of the eye spot. Beginning at 5-6 days of development, the

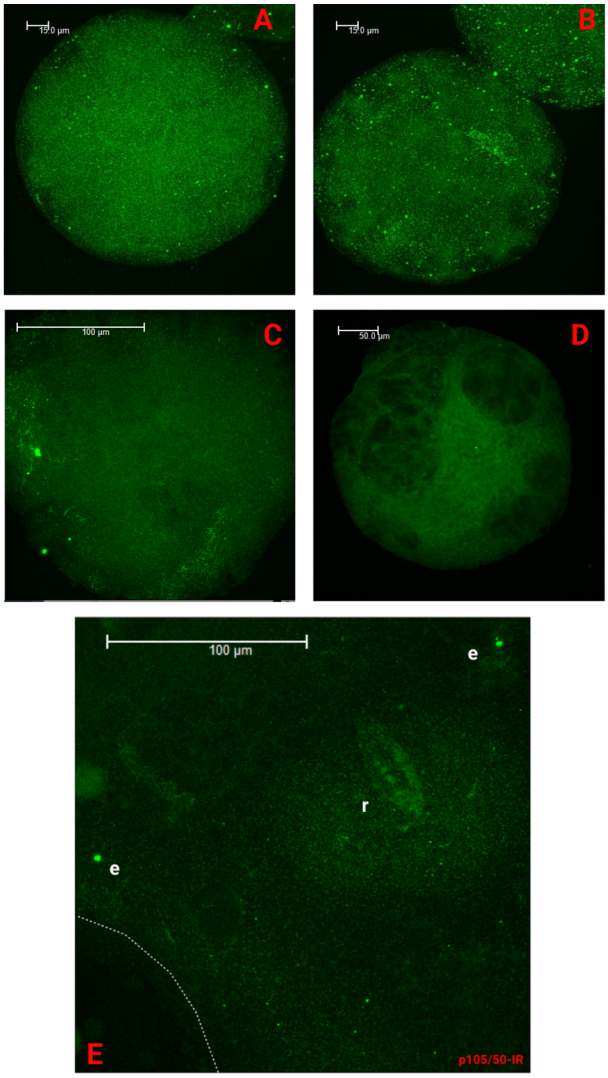

Figure 6: ***Confocal images of 0-5 day*** **B. glabrata** ***embryos treated with anti-p105/50 antibody.*** (A) 0-1 day embryo. (B) 1-2 day embryo. (C) 2-3 day embryo. (D) 3-4 day embryo. (E) Green=p105/50-IR in a 4-5 day embryo. e=eye. r=radula. Dashed line indicates edge of specimen. (A-D) exhibited no specific p105/50-IR. 4-5 day embryos in (E), however, consistently showed p105/50-IR patterns in the eye spots. All p105/50-IR patterns presented were observed in at least 20 embryos between 4-5 days of development.

eye spot became more distinguishable by the development of pigmented cells encircling the center of the eye, which continued to express strong p105/50-IR (Figs. 7, 10B). In addition to p105/50-IR within the eyespot, at 5-6 days of development p105/50-IR localized in immunoreactive structures within the headfoot region. These structures were typically found between the two eyespots and near the anterior of the headfoot (Fig. 7). Another structure showing p105/50-IR in 5-6 day embryos was a thin, elongated shape that extended from the edge of the shell opening, stopping approximately between the eye spots (Fig. 7).[5]

Localization of p105/50-IR in the eye spot continued into later stages of development, with 6-7 day embryos exhibiting fluorescence in the eyes as well (Figs. 8, 10C). In addition to fluorescence in the eye spot, notable p105/50-IR in 6-7 day embryos was seen in large structures that were clustered together just beneath the shell-headfoot interface (Fig. 8). Further, another structure demonstrating p105/50-IR in 6-7 day embryos was an elongated line of fluorescence beginning at the opening of the shell (Fig. 8A), which was also observed in 5-6 day embryos (Fig. 7). This structure was seen to extend further along the headfoot region than in 5-6 day embryos because it stretched to the edge of the specimen rather than stop between two eye spots near the radula (Fig. 7). In a ventral layer of tissue near the bottom of the headfoot, p105/50-IR was also observed in elongated lines crossing obliquely with the appearance of muscle (Fig. 9). This pattern of IR was observed throughout a majority of the headfoot region in 6-7 day embryos (Fig. 9A), however, the p105/50-IR was most prominent and clear in the area between the radula and eyespot (Fig. 9B). [6]

[5] For an additional image of a 5-6 day embryo expressing p105/50-IR, see Appendix II: Supplementary Immunofluorescence Images

[6] For additional images of 6-7 day embryos expressing p105/50-IR, see Appendix II: Supplementary Immunofluorescence Images

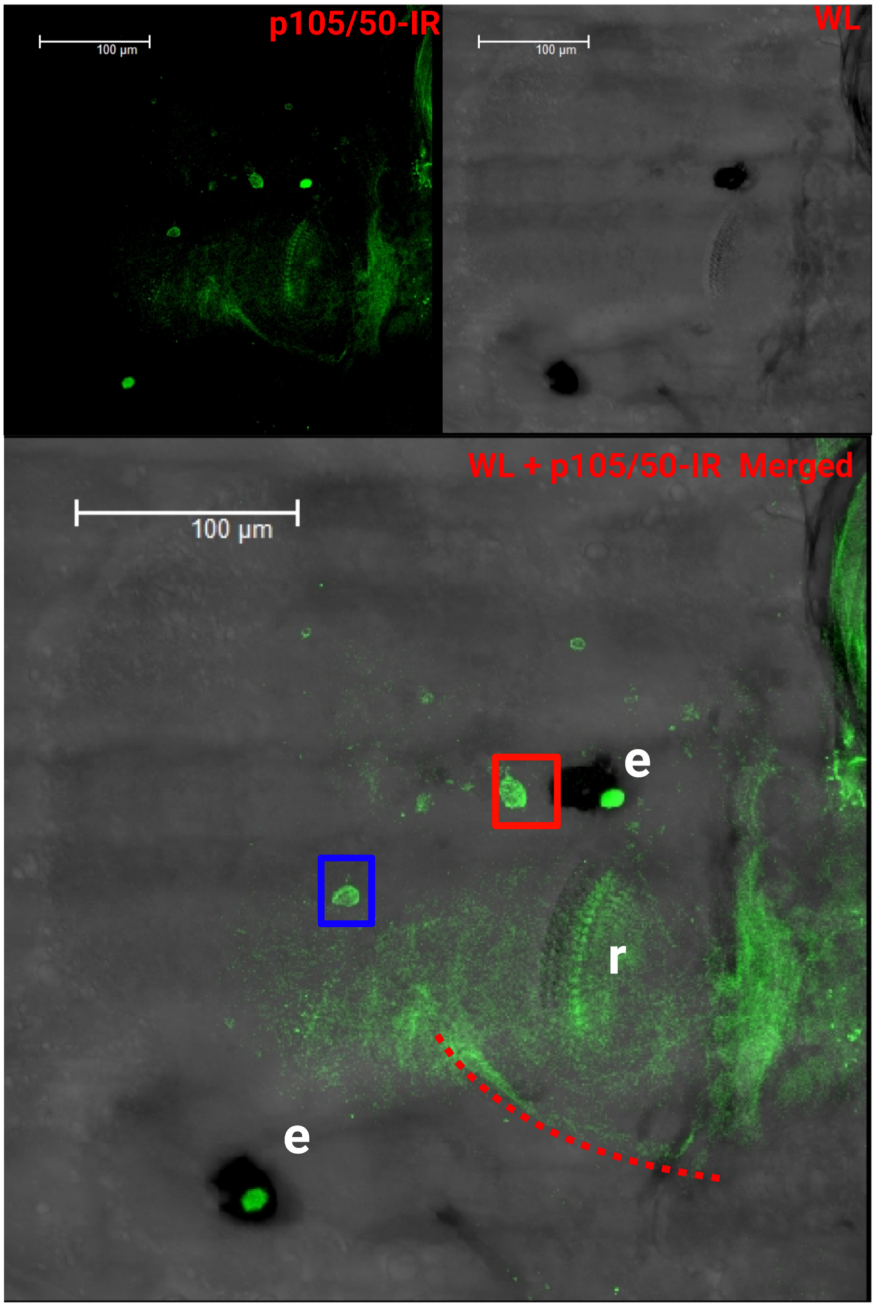

Figure 7: ***p105/50-IR in a 5-6 day*** **B. glabrata** ***embryo.*** e=eye spot. r=radula. Green=p105/50-IR. White light (WL) confocal images and p105/50-IR confocal images were merged to produce a single composite image. Dashed red line follows the path of a thin structure extending half the length of the headfoot region and ending between the eye spots. Red and blue boxes indicate additional immunoreactive structures. All p105/50-IR patterns presented were observed in at least 30 embryos between 5-6 days of development.

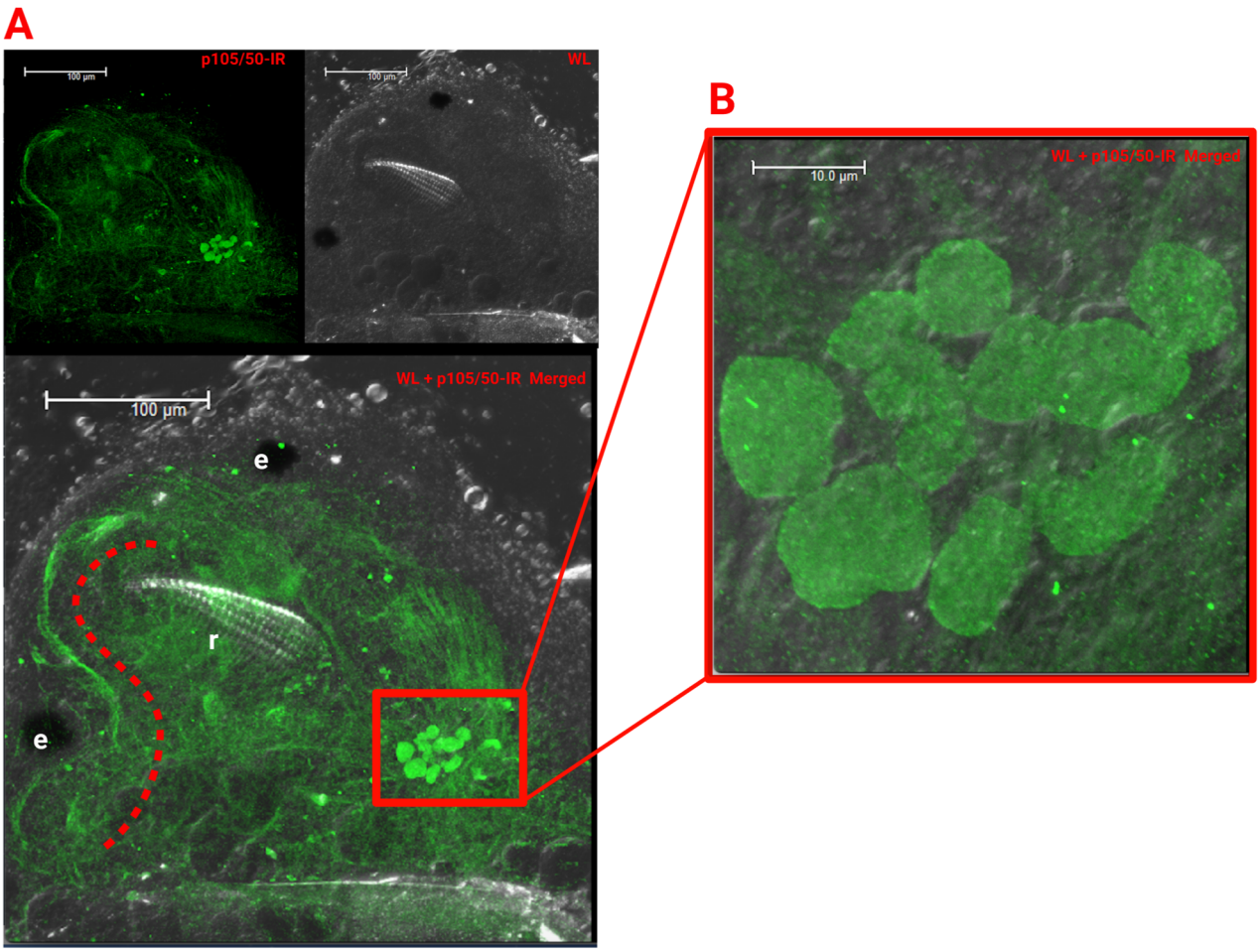

Figure 8*: p105/50-IR in a 6-7 day* B. glabrata *embryo*. e=eye spot. r=radula. Green=p105/50-IR. (A) White light (WL) confocal images and p105/50-IR confocal images were merged to produce a single composite image. Dashed red line follows the path of a thin structure extending the length of the headfoot between the eye spots. Immunoreactive structures indicated by red box and magnified. (B) Max projection of magnified immunoreactive structures.

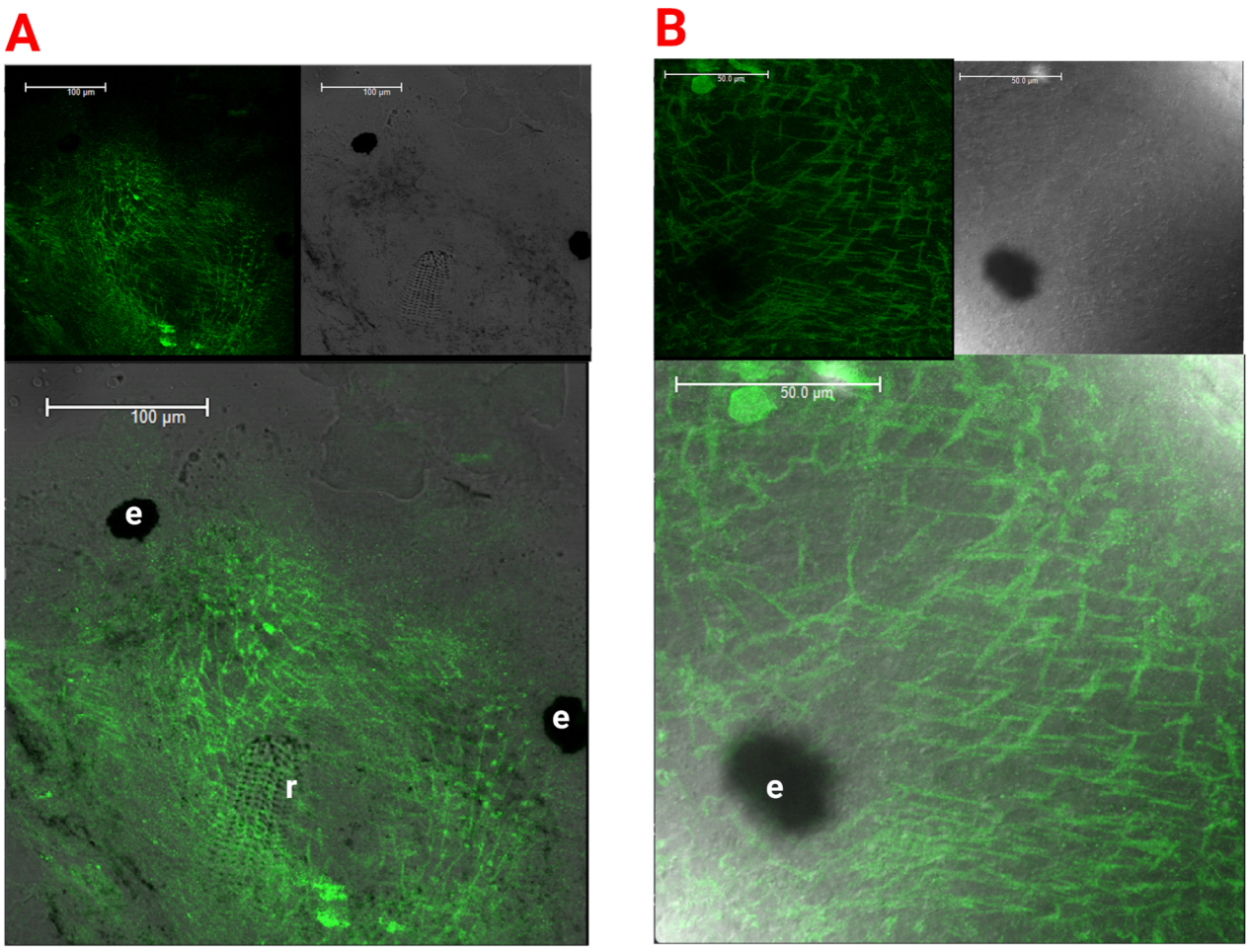

Figure 9: ***Lower layers of 6-7 day embryonic*** **B. glabrata** ***tissue expressing p105/50-IR.*** e=eye. r=radula. Green=p105/50-IR. White light (WL) confocal images and p105/50-IR confocal images were merged to produce a single composite image. Note that the eyespot does not show active p105/50-IR in same layer as muscle-like localization in the images. (A) Headfoot region of a 6-7 day embryo expressing p105/50-IR. (B) Tissue surrounding the eye spot of a 6-7 day embryo expressing p105/50-IR.

One of the most prominent and consistent findings from this study was the localization of p105/50-IR in the eye spots of embryos between 4-7 days of development. Results showed that prior to 5 days of development the eye spots were difficult to recognize when viewed under only white light, as there was no pigment surrounding the eye; rather, there was a small, concave area in the tissue, indicated by a white-dashed circle in Fig. 10A, that served as the only marker of the eye spot. After 5 days of development, however, a dark pigment was observed in the periphery of the eye and the eye spot grew in size, making it one of the most recognizable organs in the embryo (Fig. 10B, C).

Because p105/50-IR was seen in the eye spot of older embryos, it was of interest to confirm and investigate the presence of p105/50 in optical function and related pathways. Rhodopsin, which is a photopigment found in the retina of many animals, can be used as an indicator of photoreceptive tissue localization and therefore the eye spot. Treatment of 6-7 day embryos with anti-rhodopsin antibody showed rhodopsin-IR within the eyespots of embryos as well as a structure adjacent to the left eyespot that reached from the inside of the shell to the edge of the headfoot region (Fig. 11A, B, C). Closer inspection of this shape in 6-7 day embryos revealed an oval-shaped patch of rhodopsin-IR at headfoot end of the structure (Fig. 11B).

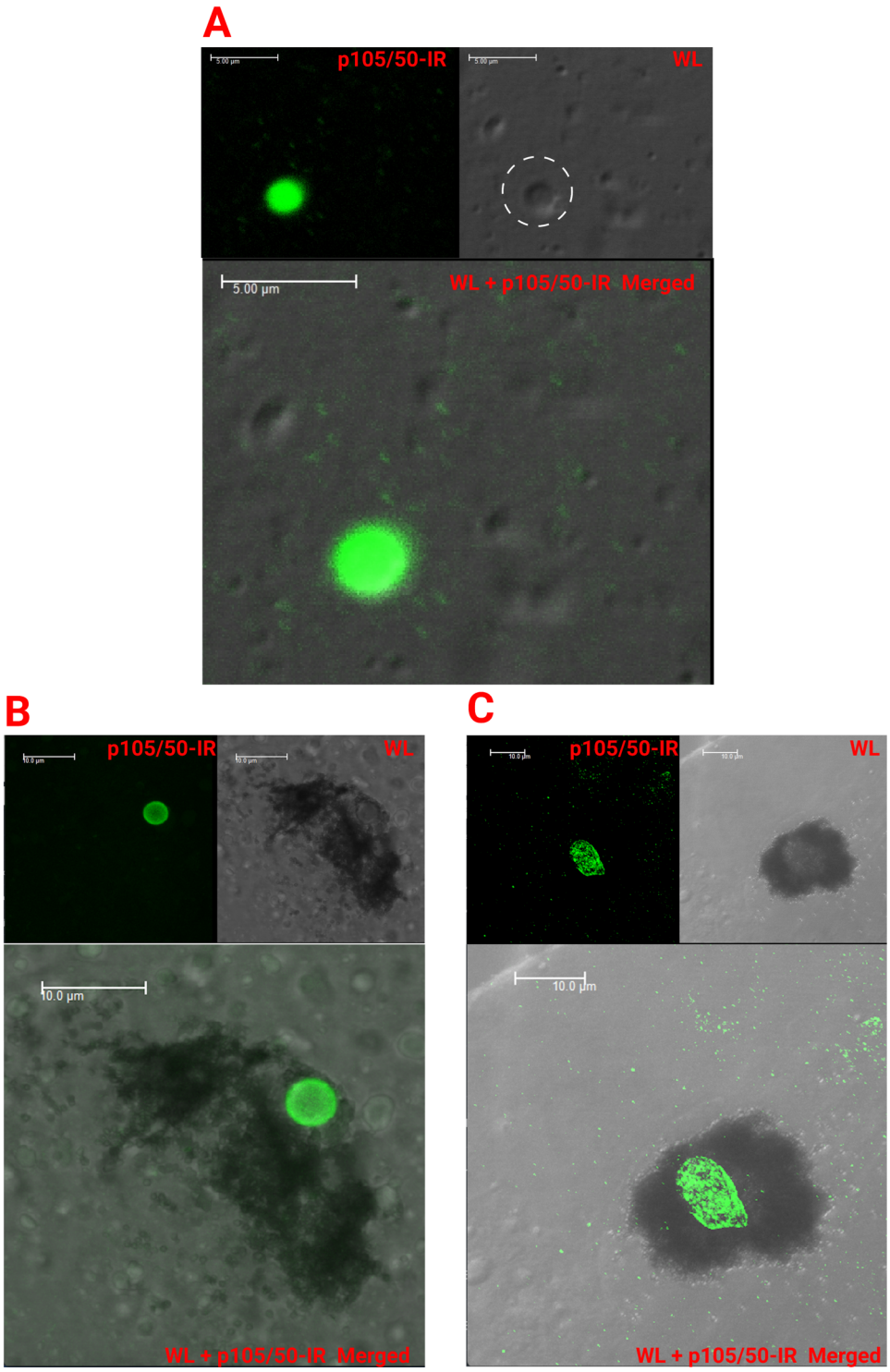

Figure 10: ***Development of*** **B. glabrata** ***eye spots exhibiting p105/50-IR.*** Green=p105/50-IR. p105/50-IR and white light (WL) confocal images were merged to produce a composite image. (A) 4-5 day embryo eye spot lacking dark pigment surrounding the area of p105/50-IR. White dashed circle indicates indent of the early eye spot. (B) 5-6 day embryo eye spot with surrounding dark pigment. (C) 6-7 day embryo eye spot with dark pigment surrounding the periphery of the eye.

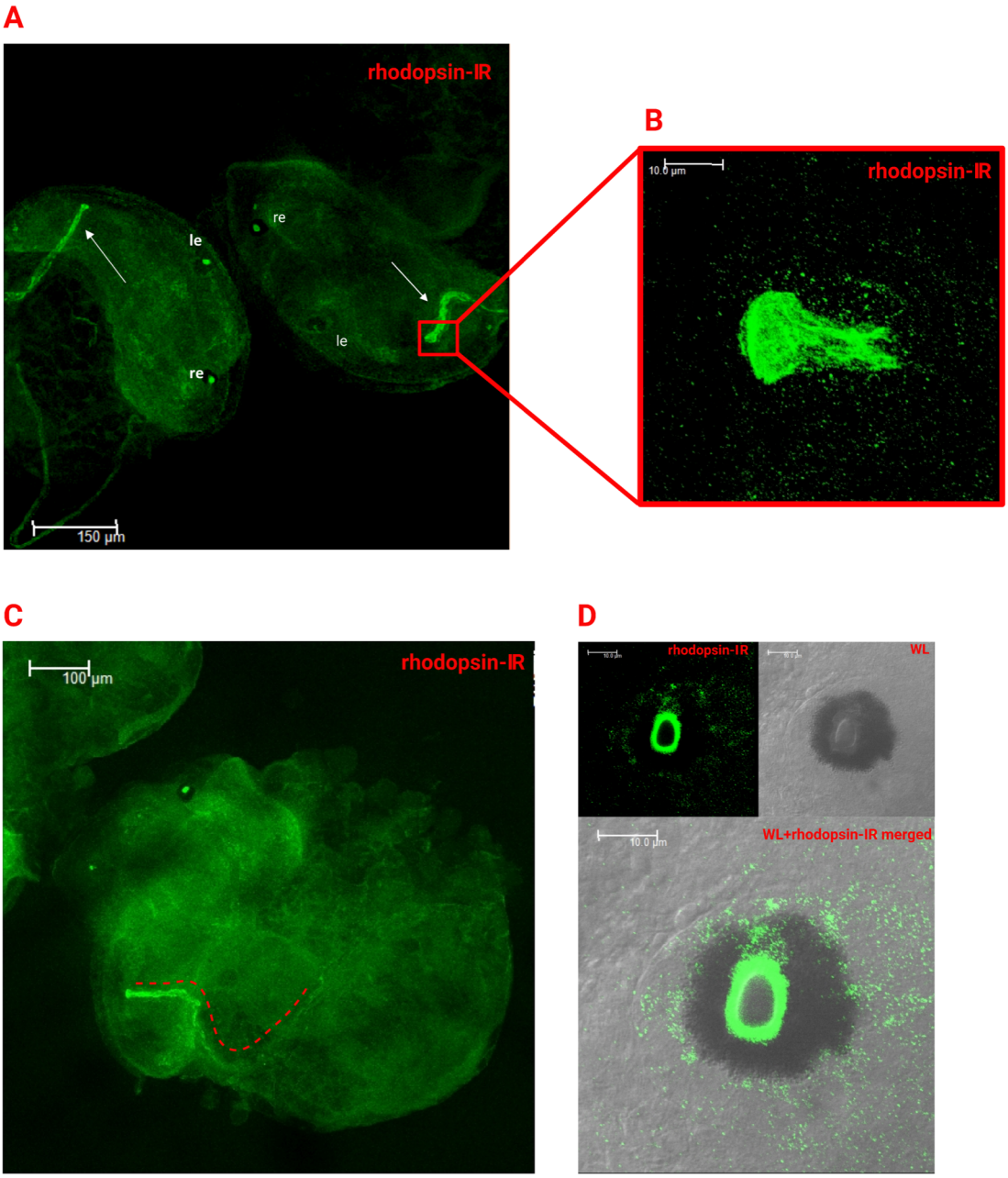

Figure 11: ***Rhodopsin-IR in 6-7 day*** **B. glabrata** ***embryos***. Green=rhodopsin-IR. (A) Pair of embryos expressing rhodopsin-IR. le= left eyespot. re=right eyespot. Elongated, tube-like structures indicated by white arrows. Red box captures end of this structure, which is magnified in (B). (C) Structure expressing rhodopsin-IR traced by a dashed red line from the headfoot into the shell. (D) Merged white light (WL) and rhodopsin-IR confocal image of a magnified eye spot expressing rhodopsin-IR. Rhodopsin-IR patterns presented were observed in at least 30 embryos between 6-7 days of development.

As both the anti-p105/50 and anti-rhodopsin antibodies were produced in rabbits, each reagent was used individually and a dual-labelling protocol was omitted. Side-by-side viewing of the eyespots of 6-7 day embryos at a higher magnification revealed rhodopsin-IR and p105/50-IR in strikingly similar areas at the center of the eye spot with dark pigmentation at the periphery of the fluorescence (Fig. 12). Additionally, closer inspection of rhodopsin-IR in *B. glabrata* eye spots showed fluorescence that was also circling the pigmented area (Fig. 12A).

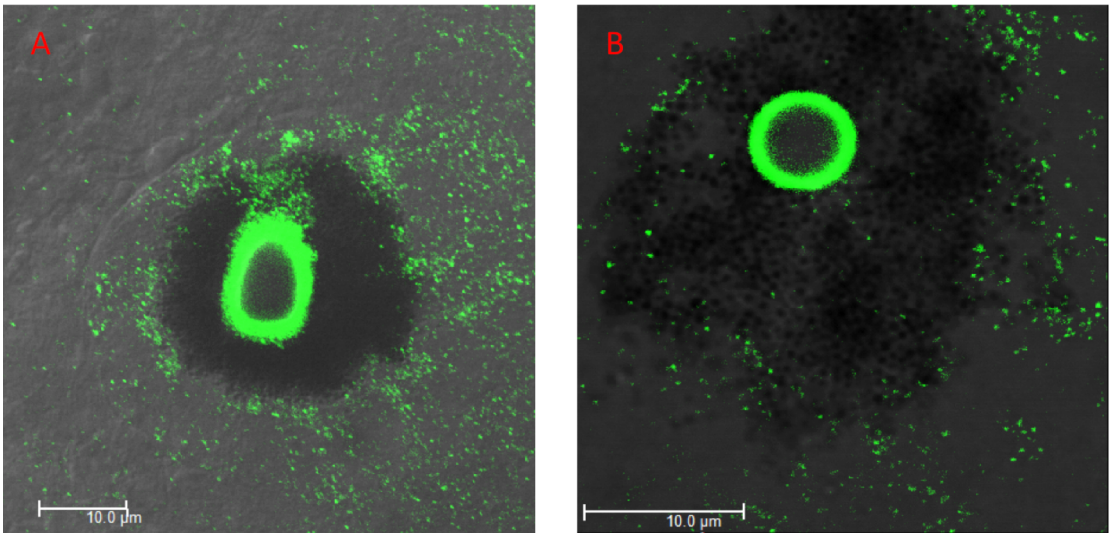

Figure 12: *Juvenile* B. glabrata *eye spots*. Merged p105/50-IR or rhodopsin-IR and WL images. (A) Green=rhodopsin-IR. (B) Green=p105/50-IR. Note that images are not max projections and capture a lower layer of the eye spot.

p105/50 and phalloidin localization in muscle-like tissue

As p105/50-IR was observed in what appeared to be muscle-like tissue, phalloidin Alexa 555, which is an actin-binding fluorescent reagent, was used to characterize this tissue as actin is an integral protein in muscle. Because of concern that there might be overlap between the emission spectra of Alexa 555 and anti-rabbit Alexa 488, embryos were treated separately with each reagent and localization patterns were

compared. Both p105/50-IR and phalloidin localized in the form of lines crossing obliquely in a similar region between the radula and the right eye (Fig. 13).

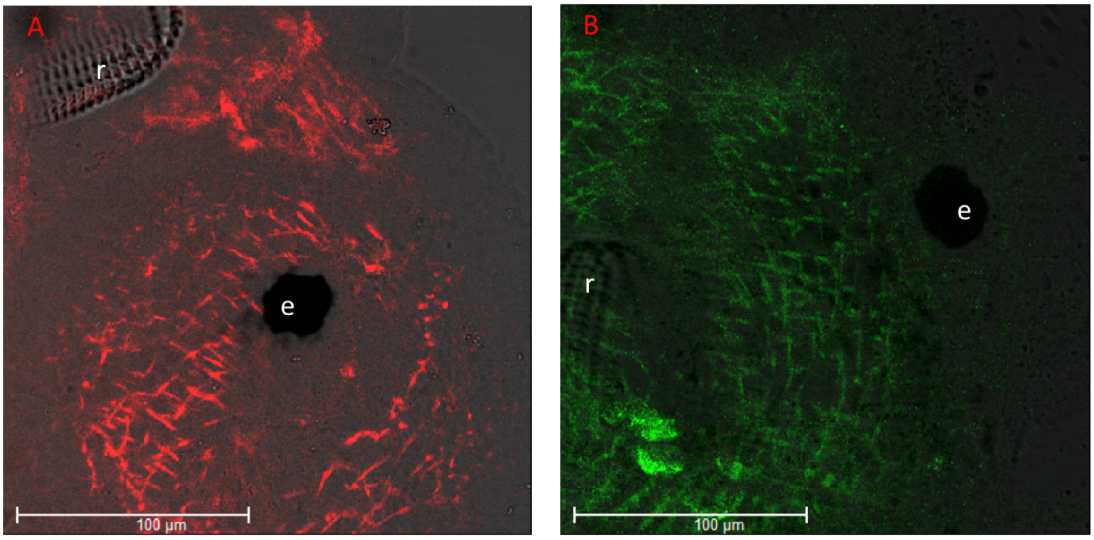

Figure 13: ***Phalloidin and p105/50 localization in juvenile*** **B. glabrata** ***embryos*****.** e=eye spot. r=radula. (A) Red=phalloidin-IR. (B) Green=p105/50-IR. Note that the eyespot does not show active p105/50-IR in same layer as possible muscle localization in the image.

Control Groups

To confirm that the observed p105/50-IR and rhodopsin-IR seen were specific, embryos were incubated with only anti-rabbit Alexa 488 (secondary treatment). Secondary only incubation did not reveal any immunoreactivity, with only the radula and shell auto-fluorescing.[7]

[7] See Appendix II: Supplementary Immunofluorescence Images for confocal image of control group.

Western Blotting

To confirm the specificity of p105/50-IR observed in *B. glabrata* embryos and to monitor p105/50 expression levels throughout the snail's development, western blotting was used. Because p105/50-IR was seen beginning at 4-5 days of development, only embryos 2-7 days developed were examined for p105/50 expression via blotting. It is important to note that the recombinant *B. glabrata* p105/50 protein terminates upstream of the p105 cleavage site and is therefore a smaller size than the native p50 protein found in embryonic and adult *B. glabrata* samples.

Only a single band slightly below 50 kD was detected in the recombinant *B. glabrata* p105/50 protein sample as expected (Fig. 14A). 3-7 day embryos showed bands at 50kD (Fig. 14A), the predicted size of native *B. glabrata* p50. While p105/50 immunofluorescence was not seen at 3-4 days of development, a faint band was observed at 50 kD at this time point on the western blot. 2-3 day embryos did not show a band at 50kD (Fig. 14A). In order to quantify and compare p105/50 expression levels, band density at each embryonic stage was compared to adult band density in ImageJ (Fig. 14B). Results showed that the band density relative to that of the adult increased at each stage of development after 3-4 days post-fertilization (Fig. 14B). While embryonic p105/50 expression levels were greatest at 6-7 days of development, adult expression was still about twice as high in comparison. Nonspecific reactivity was present in all lanes except that of recombinant p105/50 protein (Fig. 14A).

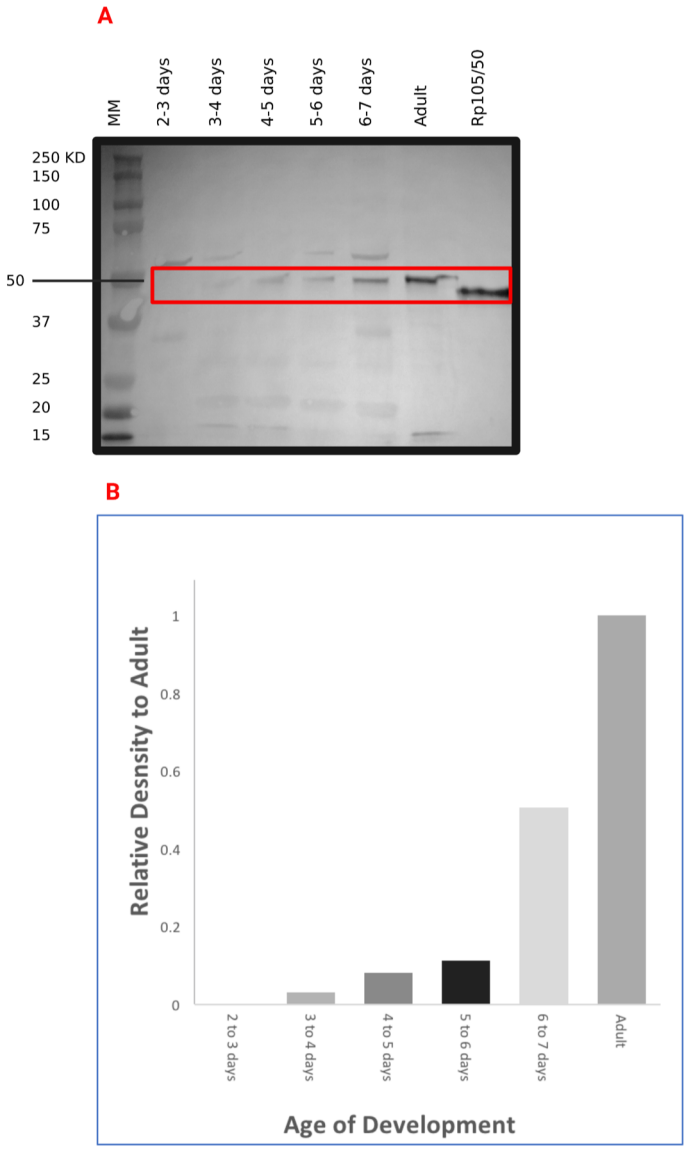

Figure 14: ***Western blotting and quantification of 2-7 day embryonic, adult, and recombinant p105/50 protein (Rp105/50) samples.*** (A) Western blot of collected samples. MM=molecular marker. Red box indicates bands at 50kD or for Rp105/50, slightly below 50kD. (B) Quantification of embryonic band density relative to the adult band density. n=1. Quantification conducted in ImageJ.

Discussion

In this study, p105/50 NF-κB protein was discovered to localize in *B. glabrata* during embryonic development. Prior to this research, NF-κB was only known to be in adult *B. glabrata*, making the results of this research a novel addition to the growing knowledge surrounding *B. glabrata* NF-κBs.

p105/50 localizes in the eye spots of B. glabrata *embryos*

One of the most significant findings from this study was p105/50-IR in the eye spot of 4-7 day *B. glabrata* embryos (Fig. 10). To confirm that p105/50 was in fact localized in the *B. glabrata* embryonic eye spot, we utilized an anti-rhodopsin antibody as rhodopsin is found in the retina of most animals. While rhodopsin has yet to be identified and characterized in *B. glabrata*, the rhodopsin antibody used in this study was successful in detecting rhodopsin in *L. stagnalis* in areas such as the photoreceptive layer near the lens (Takigami *et al.*, 2014). Given that *L. stagnalis* and *B. glabrata,* are in the same class*,* it was expected that treatment with the same rhodopsin antibody would produce similar results.

The *B. glabrata* eye has not yet been studied extensively; however, Baptista and Schall (1989) did characterize and diagram the snail's adult eye, giving insight into the functional components of the organ. *B. glabrata* eyes can be organized by four general structures: the lens, retina, optic nerve, and cornea. The lens is the most distinct portion of the eye, with its large, circular shape residing in the center of the eyespot. Dorsal to the lens is the cornea, which only covers the exposed portions of the lens that are not surrounded by the retinal layers. The optic nerve is ventral to the lens and extends into the nervous system. The retina is one of the more complex aspects of the eye, as it is divided into four distinct layers: the pigmented layer, photoreceptive layer, nuclear layer, and fibrous layer (Bapista and Schall, 1989; Fig. 15). While *B. glabrata* and *L. stagnalis* share a similar eye structure, only the *L. stagnalis* eye has characterized rhodopsin localization. In a *L. stagnalis* adult eye that was stained with anti-rhodopsin antibody by Takigami *et al.* (2014), a pear-shaped eye and a strikingly dark pigmented layer are the most profound similarities between the two species. A notable discovery from Takigami *et al.* (2014) was

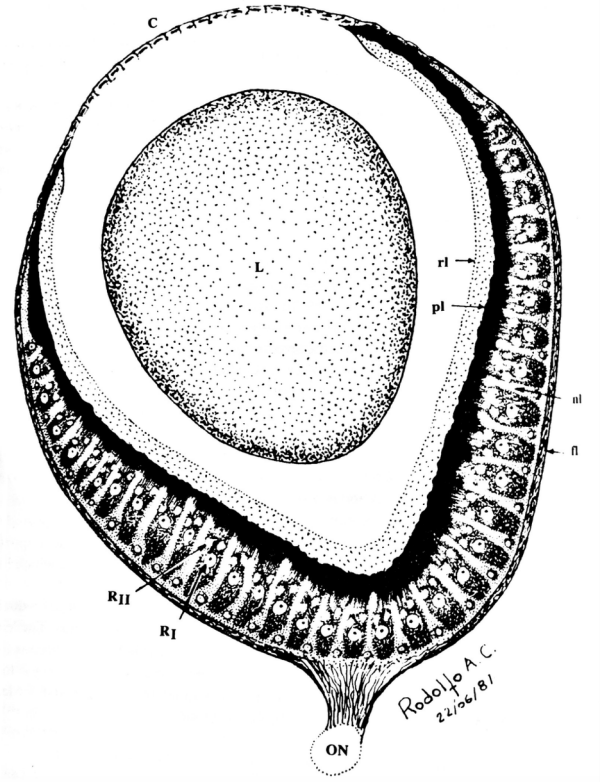

Figure 15: ***Schematic of a transverse section the*** **B. glabrata** ***eye.*** L=lens. C=cornea. ON=optic nerve. pl=pigmented layer. rl=photoreceptive layer. nl=nuclear layer. fl=fibrous layer. R_I=type I receptor. R_{II}=type II receptor. Adapted from Baptista, D. and Schall, V. (1989).

that they found a photoreceptive layer close to the lens, more specifically the "rhabdomeric membrane," to be one of several locations positive for rhodopsin (Fig. 16).

Looking at the rhodopsin-IR of a 6-7 day *B. glabrata* embryo, the most intense fluorescence is seen within the center of the pigmentation of the surrounding area (Fig. 11D), making it likely that rhodopsin at the very least localizes in one of the retinal layers of the embryonic *B. glabrata* eye as it does in *L. stagnalis*. It is possible that this darker, pigmented area characterizing the eye

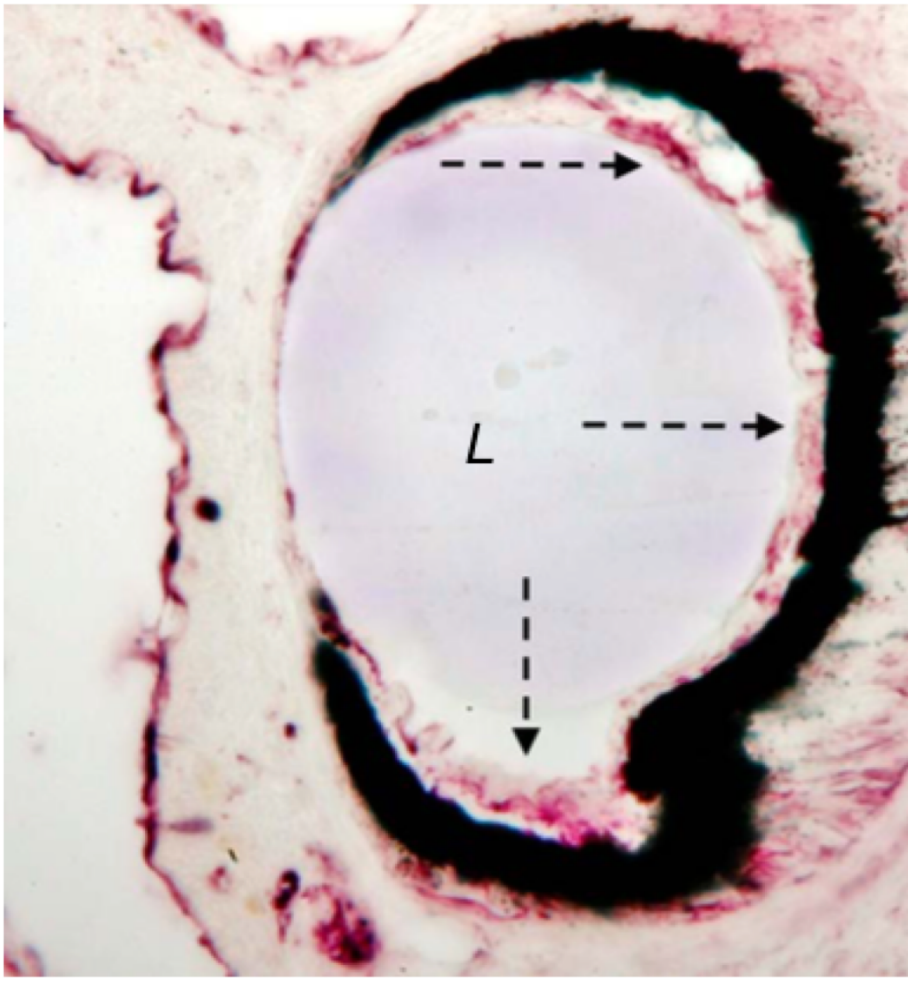

Figure 16: ***Anti-rhodopsin antibody staining of an adult*** **L. stagnalis** ***eye.*** L=lens. Black=pigmented layer. Positive rhodopsin staining (pink) in rhabdomeric membrane indicated by dashed arrows. Adapted from Takigami *et al.* (2014).

spot is the early stages of the pigmented layer of the eye forming, but studies examining *B. glabrata* eye growth and development would need to be conducted to confirm this hypothesis.

Identification of p105/50 and rhodopsin in *B. glabrata* eye spots is a novel finding, and the similarities in the localization of each protein is striking. Both p105/50-IR and rhodopsin-IR were found to form a ring of fluorescence in the center of the eye spot (Fig. 12), making it plausible that p105/50 also localizes in the retina where rhodopsin is found. The research regarding NF-κB in relation to photoreception or optics is limited; however, based on recent literature focusing on NF-κB retinal functions in vertebrates, it is perhaps not unexpected that p105/50 localizes in the eye spot of *B. glabrata.* In vertebrates, p50 is one of the most widely expressed NF-κB proteins in the retina of mice, for example (Fan and Cooper, 2009). There is also evidence that NF-κB plays a role in vertebrate retinal maintenance (Zeng *et al*., 2008). This could explain the presence of p105/50-IR in the eye spots during the later stages of embryonic development; however, this idea will have to be further investigated. Nonetheless, these results appear to be the first report of NF-κB localization in an invertebrate eye.

While rhodopsin and p105/50 demonstrated similar localization in the eye spot of all embryos between the ages of 6-7 days (Fig. 12), rhodopsin-IR was also expressed in an unknown structure outside of the eye spot that extended from the edge of the headfoot region into the inside of the shell (Fig. 11C). Rhodopsin is best known for its role in visual function, however, studies have suggested that rhodopsin also functions extra-ocularly, or outside the retina. For example, the deep-sea squid *Todarodes pacificus* contained rhodopsin in the parolfactory vesicles. Despite being outside of the eye, rhodopsin nonetheless was hypothesized to be involved in

photoreception (Hara and Hara, 1980). Furthermore, in *Drosophila,* rhodopsin was found to function completely independent from light, instead participating in a thermosensory pathway that regulates the fly's temperature sensitivity (Shen *et al.*, 2011). Thus, the additional staining of a long, tubular-like structure outside of the eye spot in 6-7 day embryos (Fig. 11A, B, C) may be an indication that *B. glabarata* rhodopsin plays a role outside of the visual system. The possible identity of this structure may also be related to respiration, as rhodopsin activity was positive in the pneumostome, a respiratory pore unique to slugs and snails, of *L. stagnalis* in previous experiments (Takigami *et al.*, 2014). Since *L. stagnalis* and *B. glabrata* share a similar respiratory system, it is possible that there is in turn similar reactivity in that area in *B. glabrata.*

p105/50 localizes in B. glabrata *embryonic muscle-like tissue*

In addition to distinct eye spot staining, anti-p105/50-IR revealed muscle-like structures between the radula and right eyespot in embryos close to hatching when viewed under a higher magnification (Figs. 9B, 13B). It was hypothesized that p105/50-IR was in the muscle primarily because the fluorescent patterns were elongated and repetitive, much like muscle cells, which contain actin filaments that are essential to locomotive function. The "foot" of *B. glabrata* is particularly muscle-dense, as movement results from a wave-like movement of muscle contractions (Lai *et al.,* 2010), so it is not unexpected to find muscle in this area of the embryo. To support the hypothesis that p105/50 was localizing in muscle, an actin binding reagent, Alexa 555 phalloidin, was used to compare to p105/50-IR. As noted in the results, there was concern that the emission spectra of Alexa 555 phalloidin and anti-rabbit Alexa 488, which bound to the p105/50 antibody, were deemed to be too close together to conduct dual staining as excitation of

both fluorophores simultaneously could result in cross-over results. By imaging embryos with only Alexa 555 phalloidin or anti-rabbit Alexa 488, it was ensured that confocal images were only capturing the fluorescence of one fluorophore. When observing the area surrounding the right eyespot of embryos treated with Alexa 555 phalloidin or anti-p105/50 antibody, there were striking similarities between the two (Fig. 13). In particular, p105/50-IR and phalloidin binding were extremely similar to one another in that both showed patterns of fluorescent lines crossing obliquely (Fig. 13), a classic indication of muscle cells. Further, anatomical studies of the *L. stagnalis* muscular system, which is likely similar to *B. glabrata*, found both smooth and striated muscle within the organism (Plesch, 1977). As such, it is extremely likely that p105/50 localizes in *B. glabrata* muscle based on the location of p105/50-IR.

While studies on NF-κB in invertebrate muscle are lacking, promising research in vertebrates have suggested that the transcription factor is important to muscle maintenance and development. In a vertebrate C212 skeletal muscle cell line, NF-κB was identified in the nuclei and was found to be involved in embryonic muscle cell proliferation and halting cellular differentiation in invertebrates (Guttrich *et al*., 1999), suggesting that NF-κB is critical for early muscular-development. In the medical field, NF-κB is also being examined for its involvement in vertebrate muscle repair, with evidence of the transcription factor being activated in patients with various forms of muscular defects, such as polymyositis and Duchenne muscular dystrophy (Monici *et al*., 2003).

Possible NF-κB localization the CNS of B. glabrata *embryos*

In addition to several large structures observed in days 5-6 post-laying (Fig. 7), a distinct cluster of structures expressing p105/50-IR was observed in 6-7 day embryos near the shell-headfoot interface (Fig. 8). While the identity of these structures is not known, it is possible that they might be involved in the CNS of the snail. One reason this may true is that preliminary studies of adult *B. glabrata* brains showed p105/50 immunofluorescence (Judith Humphries, PhD, personal communication), an indicator that p105/50 in turn may also be expressed in the developing CNS. During embryogenesis, Weinlander (2012) found serotonin (5-HT), a neurotransmitter, to localize in an elongated structure identified to be neurites near the edge of the headfoot region that was similar to the p105/50-IR found in juvenile embryos (Fig. 17). Given that 5-HT localizes in the nervous system, it is possible that similarities between p105/50-IR and 5-HT-IR in juvenile embryos suggest NF-κB might be in the *B. glabrata* nervous system (Fig 17).

While there is still uncertainty regarding the role of NF-κB in the *B. glabrata* CNS, vertebrate studies have shown that p105/50 is involved in neuronal function. Knockout p50 in mice, for example, compromised critical components of the nervous system, including pain reception, neurogenesis, and memory retention (Kassed *et al*., 2002, Niederberger *et al*., 2007, Denis-Donini *et al*., 2008, Kaltschmidt and Kaltschmidt, 2009), suggesting that p105/50 functions in neurological maintenance and function. Further, it is likely that NF-κB functions in synaptic mechanisms and neural cell proliferation in vertebrates (Kaltschmidt and Kaltschmidt, 2009).

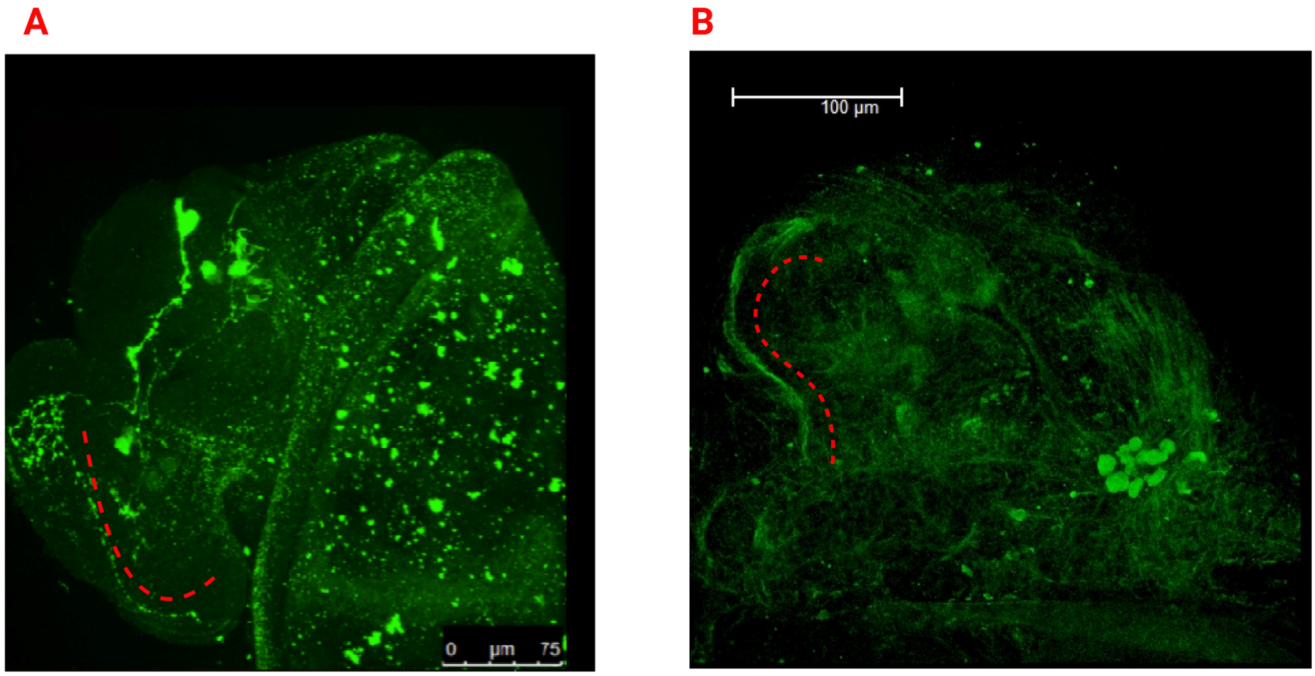

Figure 17: ***5-HT-IR and p105/50-IR in juvenile*** **B. glabrata** ***embryos.*** (A) Green=5-HT-IR. Red dashed line follows a path of 5-HT neurites. Adapted from Weinlander (2012). (B) Green=p105/50-IR. Red-dashed line indicates similar structure indicated by the red dashed line in (A).

NF-κB expression begins during B. glabrata *embryogenesis*

Like immunofluorescence, western blotting strongly suggests that p105/50 is expressed during the snail's early development. Western blotting revealed that p105/50 expression begins as early as 3-4 days of development in *B. glabrata* embryos (Fig. 14). It is important to note, however, that while western blotting indicated that p105/50 expression began at 3-4 days of development, p105/50-IR was only noticeable at 4-5 days post-fertilization.

Expression levels of embryonic p105/50 relative to that of the adult snail were seen to increase with each stage of development, suggesting that NF-κB expression also increases as *B. glabrata* matures. There were several nonspecific bands that appeared for all samples except for that of the recombinant p105/50 protein. It is possible that this was due to antibody degradation as a result of freeze-thaw cycles or simply a high primary antibody concentration, as previous western blots conducted in the Humphries Lab with the same antibody did not show nonspecific bands.

Conclusions and Future Studies:

While the findings from this research are novel regarding the localization and potential roles of NF-κB, specifically p105/50, during *B. glabrata* embryonic development, there is still a significant gap in our understanding of how p105/50 functions in the embryonic and adult snail. In this study, the localization of p105/50 in eye spots and muscle was determined using supplementary reagents known to target rhodopsin and actin. It is important to note, however, that the results produced by using reagents such as an anti-rhodopsin antibody and Alexa 555 phalloidin were novel in themselves, as neither rhodopsin or muscle development have been characterized in *B. glabrata.*

A promising area of study in *B. glabrata* regarding NF-κB functionality is in the CNS and retina of the snail. While this study provides initial evidence of p105/50 localization in the eye spots, as well as possible expression in the CNS, there are several additional steps that will need to be

taken to confirm this hypothesis. Studies will be carried out to identify the localization of p105/50 in the adult snail, as there are no published studies on NF-κB localization at any point during its lifespan. To investigate possible embryonic p105/50 localization in the CNS, it would be beneficial to optimize a dual-labeling immunofluorescence protocol using an anti-5-HT antibody with the anti-p105/50 antibody to identify points of colocalization between the IRs. Additionally, it would be beneficial to stain the nuclei of the embryos using reagents such as Hoechst or DAPI to see if the cluster of structures in 6-7 day embryos expressing p105/50-IR (Fig. 8) are cellular. Preliminary experiments using Hoechst allowed visualization of cell nuclei; however, as embryos were whole-mounted on slides for immunofluorescence, it was difficult to associate one nucleus to one cell as multiple layers of nuclei can fluoresce in the same area.

As mentioned previously, rhodopsin has yet to be characterized in *B. glabrata.* While four *B. glabrata* opsin sequences have been predicted (Ramirez *et al*., 2016), preliminary polymerase chain reaction (PCR) experiments that we conducted targeting a rhodopsin sequence failed to amplify a rhodopsin-like transcript. However, a transcript for another one of these opsins, retinochrome, was recently identified within transcript data made available through the *B. glabrata* genome project (Adema *et al*., 2017). Currently, a custom antibody against this transcript is being developed to study retinochrome further. Moving forward, it would be of interest not only to confirm the genomic sequence of rhodopsin in *B. glabrata,* but also to investigate photoreception and retinal development in the snail as a whole. Future studies will examine and potentially identify other proteins related to optics including the transcription factor PAX6, which is known to be involved in molluscan eye development (Tomarev et al., 1997).

While there are many future experiments to be conducted regarding the localization of NF-κB in *B. glabrata,* this novel study is the first to report NF-κB expression during not just gastropod development, but molluscan embryogenesis as a whole.

Acknowledgements:

As this honors thesis is the product of three years of research, I cannot express my gratitude enough to the people who have supported the growth of this project over the years.

I would most importantly like to first thank my research professor, Judith Humphries, PhD, who gave me a platform to strive for excellence not only as a student, but also as an individual. Her patience and kindness were immensely valuable as I learned how to do research independently in the lab. I was always challenged and pushed to reach the highest level of excellence in the lab, and a large part of my love for biology and science as a whole can be accredited to Judith. The three years of my Lawrence career that I spent in the Humphries lab were some of the most impactful and inspiring of my life, and I will always be grateful for having such a remarkable mentor during my undergraduate career.

Additionally, I express my deepest thanks to the entire biology department. Specifically, Biology 650 instructors, Beth De Stasio, PhD, and Amy Nottingham-Martin, who patiently guided me as I worked through this project, and Brain Piasecki, PhD, who trained me on the confocal microscope. Further, the laboratory work conducted for the experiments would not have been

possible without the Lawrence University biology department stockroom staff, who have included JoAnn Stamm, Wayne Krueger, Eric Lewellyn, PhD, and their student assistants.

I would also like to thank my peers, particularly the members of the Humphries Lab. These have included Lulu Bautista-Ruiz ‘20, who contributed immensely to documenting *B. glabrata* embryonic development, as well as Helen Threlkeld ‘22, Ben Glazer ‘23, and Marissa Zintel ‘23. I also extend my thanks to the members of the Biology 650 class, specifically Izzy Beltz ‘21, who thoughtfully read and critiqued the abstract, introduction, background, and investigative approach of this paper, which comprised my senior experience.

Finally, I express my deepest gratitude to the members of my honors project examining committee who have set aside time to review this project.

Funding:

I would like to recognize all sources of funding, for without this study could not have been possible. These include:

Chandler Senior Experience Fund (2021)

Lawrence University Summer research grant (2019)

References:

Adema, C. M. (2015). Fibrinogen-related proteins (Freps) in mollusks. *Results and Problems in Cell Differentiation*. 57, 111–129. Springer Verlag. https://doi.org/10.1007/978-3-319-20819-0_5

Adema, C. M., Hertel, L. A., Miller, R. D., & Loker, E. S. (1997). A family of fibrinogen-related proteins that precipitates parasite-derived molecules is produced by an invertebrate after infection. *Proceedings of the National Academy of Sciences*, *94*(16), 8691–8696. https://doi.org/10.1073/pnas.94.16.8691

Anthoney, N., Foldi, I., & Hidalgo, A. (2018). Toll and Toll-like receptor signaling in development. *Development (Cambridge, England)*, *145*(9), dev156018. https://doi.org/10.1242/dev.156018

Araújo, P. S., Caixeta, M. B., Brito, R. D., Gonçalves, B. B., Da Silva, S. M., Lima, E. C., . . Rocha, T. L. (2020). Molluscicidal activity of polyvinylpyrrolidone (PVP) functionalized silver nanoparticles to *Biomphalaria glabrata*: Implications for control of intermediate host snail of *Schistosoma mansoni*. *Acta Tropica,211*, 105644. doi:10.1016/j.actatropica.2020.105644

Ashour, D. S., Shohieb, Z. S. & Sarhan, N. I. (2015). Upregulation of Toll-like receptor 2 and nuclear factor-kappa B expression in experimental colonic schistosomiasis. *Journal of Advanced Research*, *6*(6), 877–884. https://doi.org/10.1016/j.jare.2014.08.004

Baeuerle, P. A. & Baltimore, D. (1989). A 65-kD subunit of active NF-KB is required for inhibition of NF-KB by IKB. *Genes Dev*. 3, 1689-1698.

Baptista, D. F. & Schall, V. T. (1989). Structural and functional analysis of the eye of *Biomphalaria glabrata*. (Mollusca, gastropoda, basommatophora). *Brazilian Journal of Medical and Biological Research*, Ribeirão Preto (22), 497-508.

Bautista-Ruiz, L. (2020). *Guide for the Embryonic Development of Biomphalaria glabrata*[PDF]. Appleton: Lawrence University.

Boyce, C. B., Tieze-Dagevos, J. W., & Larman, V. N. (1967). The susceptibility of *Biomphalaria glabrata* throughout its life-history to N-tritylmorpholine. *Bulletin of the World Health Organization*, *37*(1), 13–21.

Brennan, J., Messerschmidt, J., Williams, L., Matthews, B., Reynoso, M., & Gilmore, T.

(2017). Sea anemone model has a single Toll-like receptor that can function in pathogen detection, NF-κB signal transduction, and development. *Proceedings of the National Academy of Sciences*, *114* (47). https://doi.org/10.1073/pnas.1711530114

Camey, T., and Verdonk, N. H. (1970). The early development of the snail *Biomphalaria glabrata* (Say) and the origin of the head organs. *Netherlands Journal of Zoology, 20* (1), 93-121.

Chitsulo, L., Loverde, P., & Engels, D. (2004). Schistosomiasis. *Nature Reviews: Microbiology*, *2*(1), 12–13. https://doi.org/10.1038/nrmicro801

Cohen, S., Orian, A., & Ciechanover, A. (2001). Processing of p105 is inhibited by docking of p50 active subunits to the ankyrin repeat domain, and inhibition is alleviated by signaling via the carboxyl-terminal phosphorylation/ubiquitin-ligase binding domain. *The Journal of Biological Chemistry*, *276*(29), 26769–26776. https://doi.org/10.1074/jbc.M102448200

Colley, D. G., Bustinduy, A. L., Secor, W. E., & King, C. H. (2014). Human schistosomiasis. *Lancet (London, England)*, *383*(9936), 2253–2264. https://doi.org/10.1016/S0140-6736(13)61949-2

Croll R. P. (2009). Developing nervous systems in molluscs: navigating the twists and turns of a complex life cycle. *Brain, Behavior and Evolution*, *74*(3), 164–176. https://doi.org/10.1159/000258664

DeJong, R. J., Morgan, J. A., Paraense, W. L., Pointier, J., Amarista, M., Ayeh-Kumi, P. F., . . . Loker, E. S. (2001). Evolutionary relationships and biogeography of *Biomphalaria* (Gastropoda: Planorbidae) with implications regarding its role as host of the human bloodfluke, *Schistosoma mansoni*. *Molecular Biology and Evolution,18*(12), 2225-2239. doi:10.1093/oxfordjournals.molbev.a003769

Denis-Donini, S., Dellarole, A., Crociara, P., Francese, M. T., Bortolotto, V., Quadrato, G., Canonico, P. L., Orsetti, M., Ghi, P., Memo, M., Bonini, S. A., Ferrari-Toninelli, G., & Grilli, M. (2008). Impaired adult neurogenesis associated with short-term memory defects in NF-kappaB p50-deficient mice. *The Journal of Neuroscience*, *28*(15), 3911–3919. https://doi.org/10.1523/JNEUROSCI.0148-08.2008

De Zoysa, M., Nikapitiya, C., Oh, C., Whang, I., Lee, J. S., Jung, S. J., … Lee, J. (2010). Molecular evidence for the existence of lipopolysaccharide-induced TNF-α factor (LITAF) and Rel/NF-kB pathways in disk abalone (*Haliotis discus discus*). *Fish and Shellfish Immunology*, *28*(5–6), 754–763. https://doi.org/10.1016/j.fsi.2010.01.024

Dickson, K. M., Bhakar, A. L., & Barker, P. A. (2004). TRAF6-dependent NF-kB transcriptional activity during mouse development. *Developmental Dynamics, 231*(1), 122–127. https://doi.org/10.1002/dvdy.20110

Doenhoff, M. J., & Pica-Mattoccia, L. (2006). Praziquantel for the treatment of schistosomiasis: its use for control in areas with endemic disease and prospects for drug resistance. *Expert Review of Anti-Infective Therapy*, *4*(2), 199–210. https://doi.org/10.1586/14787210.4.2.199

Fan, W., & Cooper, N. G. (2009). Glutamate-induced NFkappaB activation in the retina. *Investigative Ophthalmology & Visual Science*, *50*(2), 917–925. https://doi.org/10.1167/iovs.08-2555

Galinier, R., Portela, J., Moné, Y., Allienne, J. F., Henri, H., Delbecq, S., Mitta, G., Gourbal, B., & Duval, D. (2013). Biomphalysin, a new β pore-forming toxin involved in *Biomphalaria glabrata* immune defense against *Schistosoma mansoni*. *PLOS Pathogens*, *9*(3), e1003216. https://doi.org/10.1371/journal.ppat.1003216

García-Arrarás, J. E., & Viruet, E. (1993). Enteric nerve fibers of holothurians are recognized by an antibody to acetylated alpha-tubulin. *Neuroscience Letters*, *157*(2), 153–156. https://doi.org/10.1016/0304-3940(93)90725-z

Gerondakis, S., & Siebenlist, U. (2010). Roles of the NF-kappaB pathway in lymphocyte development and function. *Cold Spring Harbor Perspectives in Biology*, *2*(5), a000182. https://doi.org/10.1101/cshperspect.a000182

Gilmore T. D. (2006). Introduction to NF-kappaB: players, pathways, perspectives. *Oncogene*, *25*(51), 6680–6684. https://doi.org/10.1038/sj.onc.1209954

Goodson, M. S., Kojadinovic, M., Troll, J. V., Scheetz, T. E., Casavant, T. L., Soares, M. B., & McFall-Ngai, M. J. (2005). Identifying components of the NF-kappaB pathway in the beneficial *Euprymna scolopes*-*Vibrio fischeri* light organ symbiosis. *Applied and Environmental Microbiology*, *71*(11), 6934–6946. https://doi.org/10.1128/AEM.71.11.6934-6946.2005

Guttridge, D. C., Albanese, C., Reuther, J. Y., Pestell, R. G., & Baldwin, A. S. (1999). NF-kappaB controls cell growth and differentiation through transcriptional regulation of cyclin D1. *Molecular and Cellular Biology*, *19*(8), 5785–5799. https://doi.org/10.1128/mcb.19.8.5785

Hara, T., & Hara, R. (1980). Retinochrome and rhodopsin in the extraocular photoreceptor of the squid, *Todarodes*. *The Journal of General Physiology*, *75*(1), 1–19. https://doi.org/10.1085/jgp.75.1.1

Hatada, E. N., Nieters, A., Wulczyn, F. G., Naumann, M., Meyer, R., Nucifora, G., McKeithan, T. W., & Scheidereit, C. (1992). The ankyrin repeat domains of the NF-kappa B precursor p105 and the protooncogene bcl-3 act as specific inhibitors of NF-kappa B DNA binding. *Proceedings of the National Academy of Sciences*, *89*(6), 2489–2493. https://doi.org/10.1073/pnas.89.6.2489

Hayden, M., West, A. & Ghosh, S. (2006). NF-κB and the immune response. *Oncogene* 25**,** 6758–6780. https://doi.org/10.1038/sj.onc.1209943

Hayden, M., & Ghosh, S. NF-κB in immunobiology. *Cell Res* 21, 223–244 (2011). https://doi.org/10.1038/cr.2011.13

Hong, J. W., Hendrix, D. A., Papatsenko, D., & Levine, M. S. (2008, December 23). How the Dorsal gradient works: Insights from postgenome technologies. *Proceedings of the National Academy of Sciences*, *105*(51), 20072–20076. https://doi.org/10.1073/pnas.0806476105

Humphries, J., & Deneckere, L. (2018). Characterization of a Toll-like receptor (TLR) signaling pathway *in Biomphalaria glabrata* and its potential regulation by NF-kappaB. *Developmental and Comparative Immunology*, *86*, 118–129. https://doi.org/10.1016/j.dci.2018.05.003

Humphries, J., & Harter, B. (2015). Identification of nuclear factor kappaB (NF-κB) binding motifs in *Biomphalaria glabrata*. *Developmental and Comparative Immunology*, *53*(2), 366–370. https://doi.org/10.1016/j.dci.2015.08.004

Huxford, T., & Ghosh, G. (2009). A structural guide to proteins of the NF-kappaB signaling module. *Cold Spring Harbor Perspectives in Biology*, *1*(3), a000075. https://doi.org/10.1101/cshperspect.a000075

ITIS standard Report Page: *Biomphalaria glabrata*. (n.d.). Retrieved February 03, 2021, from https://www.itis.gov/servlet/SingleRpt/SingleRpt?search_topic=TSN&search_value=76637#null

Jost, P. J., & Ruland, J. (2007). Aberrant NF-kappaB signaling in lymphoma: mechanisms, consequences, and therapeutic implications. *Blood*, *109*(7), 2700–2707. https://doi.org/10.1182/blood-2006-07-025809

Kaltschmidt, B., & Kaltschmidt, C. (2009). NF-kappaB in the nervous system. *Cold Spring Harbor Perspectives in Biology*, *1*(3), a001271. https://doi.org/10.1101/cshperspect.a001271

Kaltschmidt, C., Kaltschmidt, B., & Baeuerle, P. A. (1993). Brain synapses contain inducible forms of the transcription factor NF-kappa B. *Mechanisms of Development*, *43*(2-3), 135–147. https://doi.org/10.1016/0925-4773(93)90031-r

Kassed, C. A., Willing, A. E., Garbuzova-Davis, S., Sanberg, P. R., & Pennypacker, K. R. (2002). Lack of NF-kappaB p50 exacerbates degeneration of hippocampal neurons after chemical exposure and impairs learning. *Experimental Neurology*, *176*(2), 277–288. https://doi.org/10.1006/exnr.2002.7967

Kawai, T., & Akira, S. (2007). Signaling to NF-κB by Toll-like receptors. *Trends in Molecular Medicine*, *13*(11), 460–469. https://doi.org/10.1016/j.molmed.2007.09.002

Kenny, N. J., Truchado-García, M., & Grande, C. (2016). Deep, multi-stage transcriptome of the schistosomiasis vector *Biomphalaria glabrata* provides platform for understanding molluscan disease-related pathways. *BMC Infectious Diseases*, *16*(1), 618. https://doi.org/10.1186/s12879-016-1944-x

Kuroda, R., & Abe, M. (2020). The pond snail *Lymnaea stagnalis*. *EvoDevo,11*(1). doi:10.1186/s13227-020-00169-4

Lai, J. H., del Alamo, J. C., Rodríguez-Rodríguez, J., & Lasheras, J. C. (2010). The mechanics of the adhesive locomotion of terrestrial gastropods. *The Journal of Experimental Biology*, *213*(Pt 22), 3920–3933. https://doi.org/10.1242/jeb.046706

Lawrence T. (2009). The nuclear factor NF-kappaB pathway in inflammation. *Cold Spring Harbor Perspectives in Biology*, *1*(6), a001651. https://doi.org/10.1101/cshperspect.a001651

Li, Q., & Verma, I. M. (2002). NF-κB regulation in the immune system. *Nature Reviews Immunology*. https://doi.org/10.1038/nri910

Liu, T., Zhang, L., Joo, D., & Sun, S. C. (2017). NF-κB signaling in inflammation. *Signal Transduction and Targeted Therapy*, *2*, 17023–. https://doi.org/10.1038/sigtrans.2017.23

Mari, L., Gatto, M., Ciddio, M., Dia, E. D., Sokolow, S. H., De Leo, G. A., & Casagrandi, R. (2017). Big-data-driven modeling unveils country-wide drivers of endemic schistosomiasis. *Scientific Reports*, *7*(1), 489. https://doi.org/10.1038/s41598-017-00493-1

Meberg, P. J., Kinney, W. R., Valcourt, E. G., & Routtenberg, A. (1996). Gene expression of the transcription factor NF-kappa B in hippocampus: regulation by synaptic activity. *Brain Research: Molecular Brain Research*, *38*(2), 179–190. https://doi.org/10.1016/0169-328x(95)00229-l

Meffert, M. K., Chang, J. M., Wiltgen, B. J., Fanselow, M. S., & Baltimore, D. (2003). NF-kappa B functions in synaptic signaling and behavior. *Nature Neuroscience*, *6*(10), 1072–1078. https://doi.org/10.1038/nn1110

Monici, M. C., Aguennouz, M., Mazzeo, A., Messina, C., & Vita, G. (2003). Activation of nuclear factor-kappaB in inflammatory myopathies and Duchenne muscular dystrophy. *Neurology*, *60*(6), 993–997. https://doi.org/10.1212/01.wnl.0000049913.27181.51

Montagnani, C., Kappler, C., Reichhart, J. M., & Escoubas, J. M. (2004). Cg-Rel, the first Rel/NF-kappaB homolog characterized in a mollusk, the Pacific oyster *Crassostrea gigas*. *FEBS Letters*, *561*(1-3), 75–82. https://doi.org/10.1016/S0014-5793(04)00124-3

Moorthy, A. K., Savinova, O. V., Ho, J. Q., Wang, V. Y., Vu, D., & Ghosh, G. (2006). The 20S proteasome processes NF-kappaB1 p105 into p50 in a translation-independent manner. *The EMBO Journal*, *25*(9), 1945–1956. https://doi.org/10.1038/sj.emboj.7601081

Moynagh, P. (2005). The NF-κB pathway. *Journal of Cell Science,* 118, 4389-4392.

Niederberger, E., Schmidtko, A., Gao, W., Kühlein, H., Ehnert, C., & Geisslinger, G. (2007). Impaired acute and inflammatory nociception in mice lacking the p50 subunit of NF-kappaB. *European Journal of Pharmacology*, *559*(1), 55–60. https://doi.org/10.1016/j.ejphar.2006.11.074

Overview of NF-κB pathway. (2021). Retrieved February 26, 2021, from https://www.abcam.com/research-areas/overview-of-nf-kb-signaling

Plesch B. (1977). An ultrastructural study of the musculature of the pond snail *Lymnaea stagnalis*. *Cell and Tissue Research*, *180*(3), 317–340. https://doi.org/10.1007/BF00227599

Ramirez, M. D., Pairett, A. N., Pankey, M. S., Serb, J. M., Speiser, D. I., Swafford, A. J., & Oakley, T. H. (2016). The last common ancestor of most bilaterian animals possessed at least nine opsins. *Genome Biology and Evolution*, *8*(12), 3640–3652. https://doi.org/10.1093/gbe/evw248

Rushlow, C., & Warrior, R. (1992). The rel family of proteins. *BioEssays: News and Reviews in Molecular, Cellular and Developmental Biology*, *14*(2), 89–95. https://doi.org/10.1002/bies.950140204

Saha, R. N., Jana, M., & Pahan, K. (2007). MAPK p38 regulates transcriptional activity of NF-kappaB in primary human astrocytes via acetylation of p65. *Journal of Immunology*, *179*(10), 7101–7109. https://doi.org/10.4049/jimmunol.179.10.7101

Serasanambati, M., & Chilakapati, S. R. (2016). Function of nuclear factor kappa B (NF-kB) in human diseases-a review. *South Indian Journal of Biological Sciences,2*(4), 368. doi:10.22205/sijbs/2016/v2/i4/103443

Shen, W. L., Kwon, Y., Adegbola, A. A., Luo, J., Chess, A., & Montell, C. (2011). Function of rhodopsin in temperature discrimination in *Drosophila*. *Science*, *331*(6022), 1333–1336. https://doi.org/10.1126/science.1198904

Takigami, S., Sunada, H., Horikoshi, T., & Sakakibara, M. (2014). Morphological and physiological characteristics of dermal photoreceptors in *Lymnaea stagnalis*. *Biophysics*, *10*, 77–88. https://doi.org/10.2142/biophysics.10.77

Tato, C. M., & Hunter, C. A. (2002). Host-pathogen interactions: subversion and utilization of the NF-κB pathway during infection. *Infection and Immunity,70*(7), 3311 3317. doi:10.1128/iai.70.7.3311-3317.2002

Tomarev, S. I., Callaerts, P., Kos, L., Zinovieva, R., Halder, G., Gehring, W., & Piatigorsky, J. (1997). Squid pax-6 and eye development. *Proceedings of the National Academy of Sciences, 94*(6), 2421-2426. doi:10.1073/pnas.94.6.2421

Trottein, F., Nutten, S., Angeli, V., Delerive, P., Teissier, E., Capron, A., Staels, B., & Capron, M. (1999). *Schistosoma mansoni* schistosomula reduce E-selectin and VCAM-1 expression in TNF-alpha-stimulated lung microvascular endothelial cells by interfering with the NF-kappaB pathway. *European Journal of Immunology*, *29*(11), 3691–3701. https://doi.org/10.1002/(SICI)1521-4141(199911)29:11<3691::AID-IMMU3691>3.0.CO;2-L

Weinlander, Eric (2012). 5-HT and FMRFamide in the embryonic central nervous system of *Biomphalaria glabrata*. *Lawrence University Honors Projects.* Paper 15. h9p://lux.lawrence.edu/luhp/15

Xiao, C., & Ghosh, S. (2005). NF-κB, an evolutionarily conserved mediator of immune and inflammatory responses. *Advances in Experimental Medicine and Biology*. 560, 41–45. Springer Science and Business Media Deutschland GmbH. https://doi.org/10.1007/0-387-24180-9_5

Zarubin, T., & Han, J. (2005). Activation and signaling of the p38 map kinase pathway. *Cell Research,15*(1), 11-18. doi:10.1038/sj.cr.7290257

Zeng, H. Y., Tso, M. O. M., Lai, S., & Lai, H. (2008). Activation of nuclear factor-κB during retinal degeneration in rd mice. *Molecular Vision*, *14*, 1075–1080.

Zhang, G., & Ghosh, S. (2001). Toll-like receptor-mediated NF-kappaB activation: a phylogenetically conserved paradigm in innate immunity. *The Journal of Clinical Investigation*, *107*(1), 13–19. https://doi.org/10.1172/JCI11837

Zhang, S. M., & Coultas, K. A. (2011). Identification and characterization of five transcription factors that are associated with evolutionarily conserved immune signaling pathways in the schistosome-transmitting snail *Biomphalaria glabrata*. *Molecular Immunology*, *48*(15–16), 1868–1881. https://doi.org/10.1016/j.molimm.2011.05.017

Appendix I: Methods Expanded

1. To obtain Leica TCS SP5 II confocal images of *B. glabrata* embryos expressing p105/50-IR and rhodopsin-IR, argon laser 488 was used at 6-15% capacity. Images of *B. glabrata* embryos expressing Alexa 555 phalloidin fluorescence were excited with lasers 542 and 594 at 20% capacity.

2. In order to make the recombinant *B. glabrata* p105/50 protein, DNA representing the N-terminus and RHD of *B. glabrata* p105/50 was inserted into a pET-30A(+) vector (GenScript, Piscataway, NJ). *E. coli* were then transformed with the vector and a His-tagged recombinant *B. glabrata* p105/50 protein was expressed through IPTG induction.

3. To measure protein quantity in each sample containing embryonic or adult *B. glabrata* tissue, absorbance levels of each experimental and standard sample of a known BSA concentration (Table S1) were measured in duplicate at 562nm using a POLARstar Omega plate reader (BMG Lab Tech, Cary, NC). Collected absorbance values were corrected to the absorbance of a blank sample containing pure sPBS and averaged. Absorbance levels of BSA samples were then graphed versus [BSA] to create a standard curve and best fit line. The equation of this line was then used to calculate the amount protein in each *B. glabrata* embryonic or adult sample. The volume required to contain 10µg of protein, with the exception of the recombinant p105/50 sample, which had volumes calculated to contain 2.5µg of protein, was then calculated and loaded into each well.

Vial	Volume of Diluent (µL)	Volume and Source of BSA (µL)	Final BSA Concentration (µg/mL)
A	0	300 of Stock	2000
B	125	375 of Stock	1500
C	325	325 of Stock	1000
D	175	175 of vial B dilution	750
E	325	325 of vial C dilution	500
F	325	325 of vial E dilution	250
G	325	325 of vial F dilution	125
H	400	100 of vial G dilution	25
I	400	0	0 = Blank

Table S1: *Dilution scheme for standard microplate procedure of a BCA protein assay.* The diluent used in this particular study was sPBS. Adapted from Thermo Scientific.

4. As recommended by Promega, to create the BCIP/NBT development substrate, for every 5 mL AP buffer, 33 µL of NBT (50mg/mL in 70% dimethylformamide) was added to the solution and mixed. 16.5 µL of BCIP (50mg/mL in 100% dimethylformamide) was subsequently added and mixed into the solution to create the final working substrate.

Appendix II: Supplementary Immunofluorescence Images

5. Additional confocal image of a 5-6 day embryo expressing p105/50-IR:

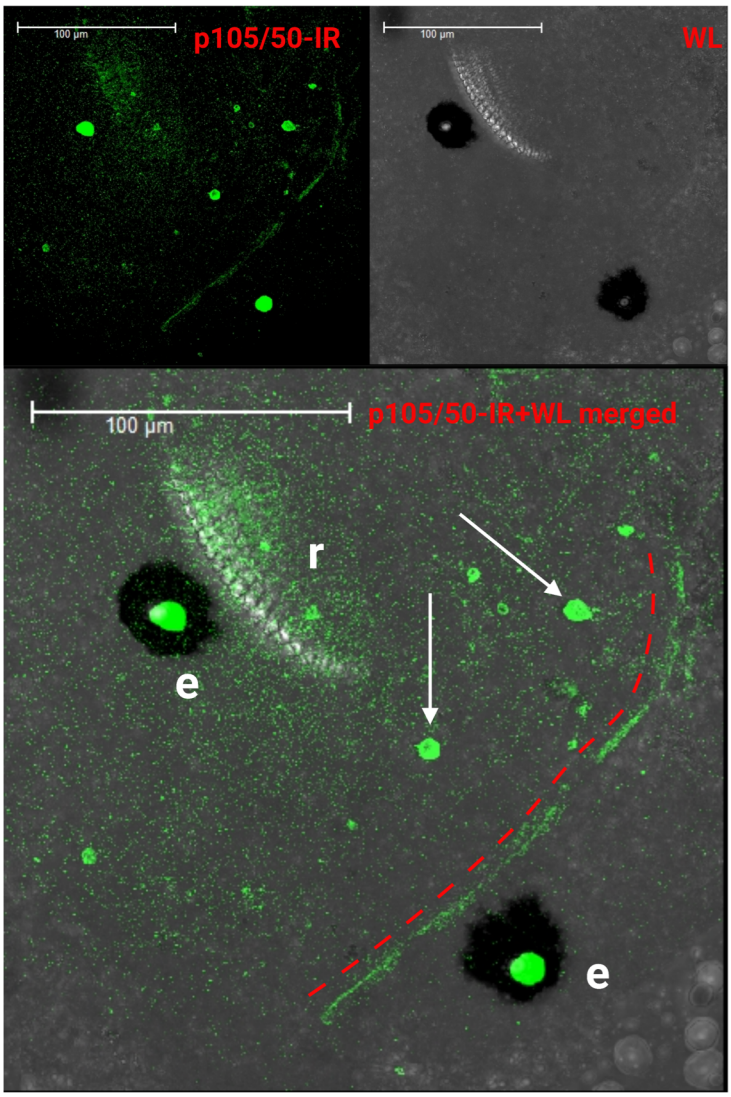

Figure S1: *5-6 day* B. glabrata *embryo expressing p105/50-IR.* e=eye spot. r=radula. White light (WL) confocal images and p105/50-IR confocal images were merged to produce a single composite image. Dashed red line follows the path of a thin structure extending between the eye spots. White arrows indicate large structures expressing p105/50-IR.

6. Additional confocal images of 6-7 day embryos expressing p105/50-IR:

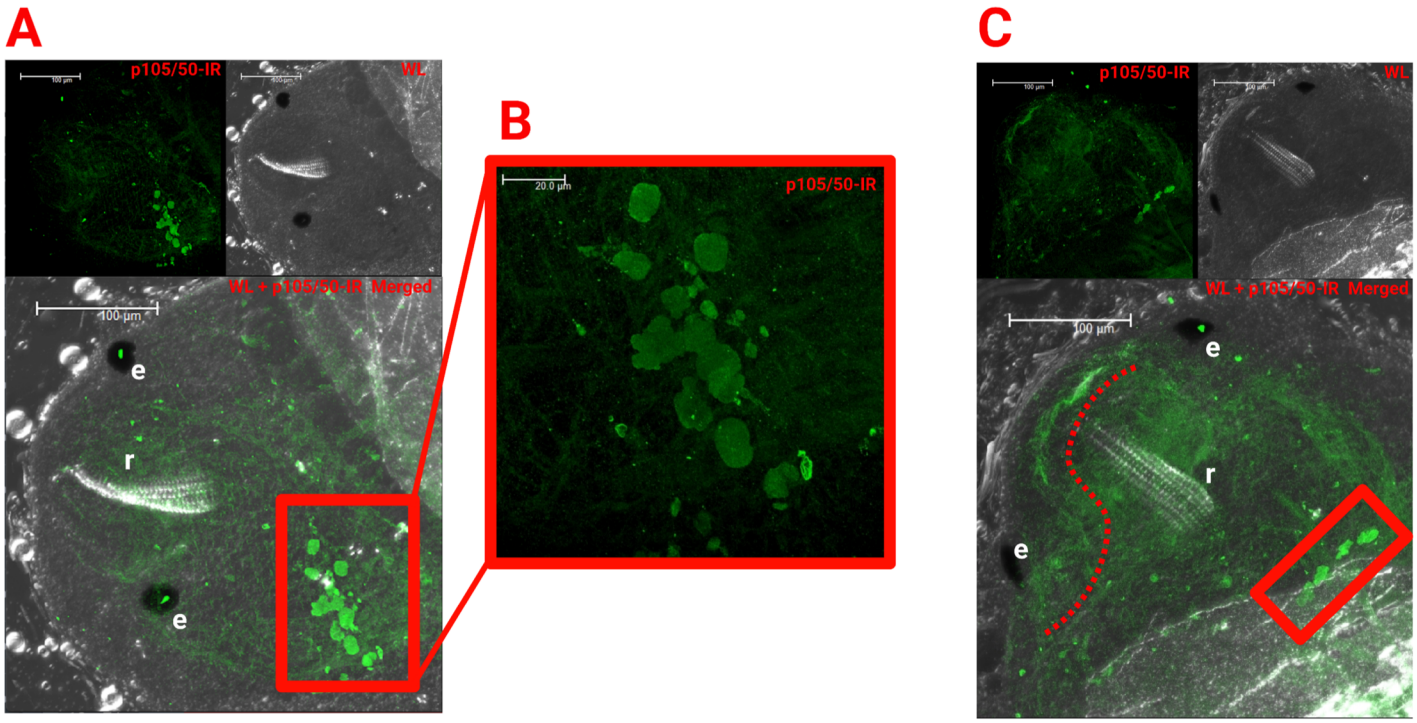

Figure S2: 6-7 day* B. glabrata *embryos expressing p105/50-IR. e=eye spot. r=radula. (A, C) White light (WL) confocal images and p105/50-IR confocal images were merged to produce a single composite image. Red boxes indicate cluster of structures expressing p105/50-IR. Dashed red line follows the path of a thin structure extending the length of the headfoot region between the eye spots. (B) Max projection of magnified cell-like structures of (A).

7. Confocal image of an embryo treated with only Alexa 488:

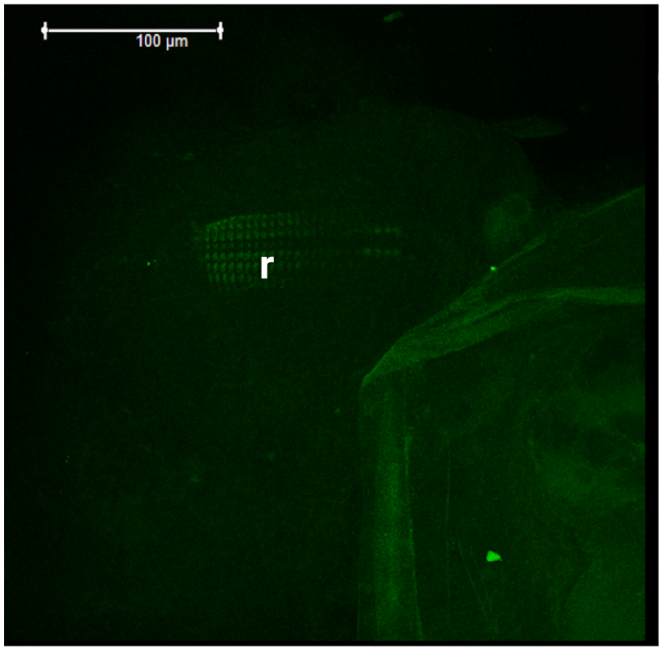

Figure S3: ***Control group of a*** **B. glabrata** ***embryo.*** r=radula. Embryo treated with only Alexa 488. The radula and shell were the only fluorescent structures in the headfoot region under this treatment.